



## Recent advances in the development of tumor microenvironment-activatable nanomotors for deep tumor penetration

Qianyang Jiang<sup>a,1</sup>, Jiahuan He<sup>a,1</sup>, Hairui Zhang<sup>b,1</sup>, Haorui Chi<sup>a</sup>, Yi Shi<sup>c,\*\*</sup>, Xiaoling Xu<sup>a,\*</sup>

<sup>a</sup> Key Laboratory of Artificial Organs and Computational Medicine in Zhejiang Province, Shulan International Medical College, Zhejiang Shuren University, Hangzhou, PR China

<sup>b</sup> School of Pharmaceutical Sciences, Zhejiang Chinese Medical University, Hangzhou, PR China

<sup>c</sup> Longhua Hospital Affiliated to Shanghai University of Traditional Chinese Medicine, Shanghai, 200032, PR China

### ARTICLE INFO

#### Keywords:

Nanomotors  
Self-propelled  
Deep tumor penetration  
Hydrogen peroxide  
Urea  
Arginine

### ABSTRACT

Cancer represents a significant threat to human health, with the use of traditional chemotherapy drugs being limited by their harsh side effects. Tumor-targeted nanocarriers have emerged as a promising solution to this problem, as they can deliver drugs directly to the tumor site, improving drug effectiveness and reducing adverse effects. However, the efficacy of most nanomedicines is hindered by poor penetration into solid tumors. Nanomotors, capable of converting various forms of energy into mechanical energy for self-propelled movement, offer a potential solution for enhancing drug delivery to deep tumor regions. External force-driven nanomotors, such as those powered by magnetic fields or ultrasound, provide precise control but often necessitate bulky and costly external equipment. Bio-driven nanomotors, propelled by sperm, macrophages, or bacteria, utilize biological molecules for self-propulsion and are well-suited to the physiological environment. However, they are constrained by limited lifespan, inadequate speed, and potential immune responses. To address these issues, nanomotors have been engineered to propel themselves forward by catalyzing intrinsic “fuel” in the tumor microenvironment. This mechanism facilitates their penetration through biological barriers, allowing them to reach deep tumor regions for targeted drug delivery. In this regard, this article provides a review of tumor microenvironment-activatable nanomotors (fueled by hydrogen peroxide, urea, arginine), and discusses their prospects and challenges in clinical translation, aiming to offer new insights for safe, efficient, and precise treatment in cancer therapy.

### 1. Introduction

According to the estimates from the International Agency for Research on Cancer (GLOBOCAN), the global incidence of new cancer cases exceeded 19.3 million in 2020, with approximately 10 million cancer-related deaths. Cancer is projected to become the leading cause of mortality worldwide in the 21st century and represents a paramount barrier to improving life expectancy globally [1]. Currently, clinical treatment methods for cancer tumors cancerous tumors often involve surgery, radiotherapy, chemotherapy, and immunotherapy [2,3]. While the various treatment modalities have improved the clinical outcomes and survival rates of cancer patients, they still face certain limitations.

Surgical intervention, characterized by short treatment cycles and rapid onset of action, is primarily efficacious for early-stage localized tumors but yields suboptimal outcomes for advanced or metastatic malignancies. Moreover, surgical procedures often necessitate delicate maneuvering to avoid vital organs, vessels, and nerves, rendering complete tumor resection challenging and potentially leaving behind risks of recurrence. Radiation therapy, although notably effective for certain tumors, carries the inherent risk of causing irreversible damage to normal musculoskeletal and neural tissues due to its inherent radiotoxicity [4]. Chemotherapy demonstrates efficacy across primary tumors, metastatic lesions, and subclinical metastases. However, it is frequently accompanied by severe side effects [5] and can foster tumor cell resistance [6].

\* Corresponding author. Shulan International Medical College, Zhejiang Shuren University, 8 Shuren Street, Hangzhou, 310015, PR China.

\*\* Corresponding author. Longhua Hospital Affiliated to Shanghai University of Traditional Chinese Medicine, 725 South WanPing Road, Shanghai, 200032, PR China.

E-mail addresses: [lh2918@shutcm.edu.cn](mailto:lh2918@shutcm.edu.cn) (Y. Shi), [ziyao1988@zju.edu.cn](mailto:ziyao1988@zju.edu.cn) (X. Xu).

<sup>1</sup> These authors contributed equally.

## 2. Emerging therapeutic modalities of cancer

### 2.1. Molecular targeted therapy

Since the late 1990s, the clinical approval and subsequent utilization of small molecule drugs or therapeutic monoclonal antibodies as signal transduction inhibitors have constituted foundational elements of precision oncology [7]. For surgical interventions, their oral administration mitigates patient discomfort, while for radiotherapy and chemotherapy, targeted action minimizes damage to normal cells. However, as clinical usage progresses, inherent drawbacks have become apparent. Primarily, efficacy is restricted to tumor patients expressing specific biomarkers. Additionally, akin to chemotherapy, molecular targeted therapy confronts challenges related to the emergence of drug resistance [8].

### 2.2. Immunotherapy

Immunotherapy, based on the activation or augmentation of the intrinsic immune system's capabilities to identify [9], attack, or induce apoptosis in tumor cells, is gradually emerging as a prominent therapeutic modality [10,11]. This approach offers the advantages of broad applicability and minimal toxic side effects. However, akin to chemotherapy, certain tumors develop resistance mechanisms, enabling evasion of immune surveillance, thereby resulting in suboptimal therapeutic efficacy [12]. Furthermore, immune-related adverse events commonly manifest in association with immunotherapy [13].

### 2.3. Multimodal therapy

#### 2.3.1. Dynamic therapy

Faced with such a large patient population and complex healthcare challenges, the limitations of current treatment methods have not changed the grim situation of cancer treatment [14]. Therefore, innovative treatment methods, leading precision medicine, breakthroughs in drug development, and other innovations can enhance our comprehensive understanding of the complexity of cancer, explore new safe treatment modalities for tumors, and provide more possibilities for efficient and safe cancer treatment. With the continuous advancement of science and technology, there are emerging new tumor treatment methods.

The so-called dynamic therapies primarily include Chemodynamic Therapy (CDT) [15], Sonodynamic Therapy (SDT) [16], Radiodynamic Therapy (RDT) [17], and Photodynamic Therapy (PDT) [18]. These therapies share a common mechanism of utilizing specific physical or chemical processes to generate reactive oxygen species (ROS) within the tumor microenvironment, thereby inducing tumor cell damage or death.

CDT exploits hydrogen peroxide ( $H_2O_2$ ) present in the tumor microenvironment to generate ROS, particularly hydroxyl radicals ( $OH\bullet$ ), through Fenton or Fenton-like reactions, inducing apoptosis in tumor cells [19]. SDT employs sonosensitizers with deep tissue penetration capability to produce ROS under ultrasonic irradiation, leading to tumor cell death [20]. Additionally, RDT typically uses X-rays or  $\gamma$ -rays to activate drugs, generating ROS to kill tumor cells [21]. PDT is a method of cancer treatment that involves activating photosensitizers with specific wavelengths of light [22]. During PDT, the photosensitizer delivered to the tumor site generates ROS upon activation by near-infrared light, resulting in tumor cell apoptosis.

However, the disadvantages of dynamic therapies are also common across these modalities, being largely constrained by the characteristics of the tumor microenvironment. The excessive expression of reducing substances within tumors, such as glutathione, can neutralize the generated ROS, thereby reducing the therapeutic efficacy [15,19].

#### 2.3.2. Photothermal therapy

In contrast to the aforementioned dynamic therapies, photothermal therapy (PTT) represents an emerging strategy for tumor treatment [23, 24]. PTT utilizes targeted recognition technology to accumulate

photothermal materials near tumor tissues. Upon excitation by near-infrared light, these materials convert light energy into heat energy, thereby selectively killing cancer cells. This method offers advantages such as minimally invasive procedures, long-lasting effects, and safety in the treatment of malignant tumors. As a result, PTT can serve as an independent treatment or an adjunct to other therapies, achieving efficient tumor inhibition and demonstrating significant developmental potential [25,26].

Although photothermal therapy has potential applications in cancer treatment, it still has some limitations. Firstly, the poor solubility of photothermal materials in water is an important factor limiting their application. Secondly, low bioavailability is also a challenge for photothermal therapy. Even if photothermal materials can be successfully injected into the tumor site, they may not be fully absorbed and utilized [27].

## 3. Limitations of nanodrug delivery systems

Targeted nanomedicine systems, due to their excellent water solubility and high bioavailability, offer a new strategy for cancer treatment. By altering the distribution of drugs in the body and increasing the permeability of biological membranes, they significantly enhance the efficacy of drugs and reduce side effects [28]. This system has shown great potential in areas such as tumors and inflammatory diseases. However, poor penetration of nanocarriers in tumor therapy is one of the important reasons limiting its development [29].

For solid tumors, the harsh microenvironment inside poses many challenges to the efficacy of nanodrugs. Firstly, the abnormal vascular permeability in tumors leads to thinning of vessel walls, facilitating fluid extravasation into the surrounding tissues, thus increasing the interstitial fluid pressure (IFP) within tumor tissues. Moreover, the densely packed tumor cells further impede fluid flow and drug diffusion, exacerbating the elevation of IFP. Additionally, the lack of effective lymphatic drainage systems in solid tumors contributes to the accumulation of interstitial fluid, another factor driving the increase in IFP [30]. Simultaneously, the loss or impairment of endothelial cell tight junction function may result in vascular inflammation and fluid extravasation, further augmenting tumor interstitial pressure [31,32]. Furthermore, the high metabolic activity of tumor cells generates a large amount of metabolic waste (such as lactate) that accumulates within the tumor, increasing local osmotic pressure. This, in turn, attracts more water into the tumor interstitium, exacerbating the elevation of interstitial pressure. These factors collectively form physical barriers that hinder the effective delivery of drugs to the interior of the tumor [33].

Secondly, tissues typically form pressure gradients, making it difficult for conventional nanopreparations to penetrate blood vessel walls and enter the depths of tumor tissues. When these targeted modified nanocarriers attempt to cross tumor blood vessels, they accumulate near the vessels by binding to receptors on the vessel walls [34].

Thirdly, as tumors grow, blood vessels grow arbitrarily and may be severed or damaged, resulting in much lower microvessel density in the center of the tumor compared to the infiltrating edge, further hindering nanoparticle delivery to the central region [35]. Despite decades of in-depth research and laboratory success, only a few nanoparticle-based small molecule cancer-targeting drugs have succeeded clinically, such as albumin nanoparticles, polymer micelles, and liposomes [36].

Therefore, in order to improve the therapeutic efficacy of nanodrugs on tumors and promote their clinical translation, it is crucial to enhance the penetration of tumor tissues and maximize the therapeutic effect in the short term [37,38]. An autonomous, drug-loaded nanorobot guided externally is considered a promising solution as it can actively navigate through hostile tumor microenvironments, further increasing drug accumulation within tumor cells and improving drug efficacy, partially alleviating drug resistance mechanisms [39], releasing anticancer drugs or responding to other types of therapy, to achieve more efficient cytotoxic effects.

#### 4. Nanomotors

At a deeper level, more active intercellular delivery becomes an ideal way for nanoparticle drug penetration [37]. An autonomous, drug-loaded nanorobot guided externally is considered a good solution because it can actively penetrate hostile tumor microenvironments, further release anticancer drugs, or respond to other types of treatment to achieve more efficient killing effects.

Nanomotors are microdevices capable of converting different forms of energy into mechanical energy, thereby achieving self-propelled propulsion [40]. This idea was initially proposed by Richard Feynman in his 1959 speech, envisioning tiny devices that could be ingested and roam through the body's blood vessels to achieve therapeutic effects [41], sparking interest in developing nanomotors as a new type of targeted drug delivery system, which in turn has driven generations of scientists and engineers to continuously expand and improve nanotechnology (Fig. 1). Compared to traditional nanomaterials, nanomotors can overcome the influence of irregular Brownian motion and break through the motion limitations of low Reynolds numbers for nanorobots [42]. Autonomous nanomotors have the ability to actively penetrate biological barriers, demonstrating superior self-driven penetration performance in dense extracellular matrices, as well as in the blood-brain barrier and blood-tumor barrier [43]. Furthermore, such powerful mobility also accelerates the uptake of anticancer drugs by lesion cells, achieving efficient drug accumulation [44]. Using nanomotors as carriers, targeted chemotherapy drugs can penetrate through layers of barriers, penetrate deep into tumors, and accomplish the important mission of efficiently inhibiting solid tumors. These outstanding advantages endow nanomotor drug delivery systems with enormous

potential applications in the field of cancer treatment, making them a remarkable frontier technology.

With the continuous expansion and refinement of nanotechnology, nanorobots are also evolving. According to the types of dynamic response to the tumor microenvironment, nanomotors can be classified into biologically hybrid [60], exogenous [61], and endogenous [62] types. Among them, biologically hybrid nanomotors use naturally motile entities with high biocompatibility (such as bacteria [63], phagocytes [64], or sperm [65]) as the development targets, which are modified using genetic engineering techniques to become "couriers" for targeted delivery of chemotherapy drugs. Akolpoglu et al. [66] found that by leveraging the strong affinity of biotin and streptavidin, nano liposomes loaded with drugs attach to the surface of *Escherichia coli*. Meanwhile, magnetic nanoparticles of photothermal agents and chemotherapy molecules also bind to *Escherichia coli*. Under the control of an external magnetic field, these "couriers" can be precisely delivered, and drug molecules can be released on demand through near-infrared stimulation.

Exogenous propulsion utilizes methods such as electric fields [67], magnetic fields [72], light [73], heat [74], or ultrasound [75] to provide energy for nanomotor movement, allowing nanomaterials to overcome the obstacles of Brownian motion. Among them, spherical FeCo nanomotors developed by Song et al. [72] have controllable motion under a magnetic field and photothermal therapy characteristics. Based on the imaging effect of Fe and the radiation damage capability of Co, they integrate cancer diagnosis and treatment, demonstrating their unique advantages. A recent study simulated a method for sound wave-driven Janus particles based on the respective advantages of photothermal therapy and sound wave propulsion [76]. Represented by Zhang et al.

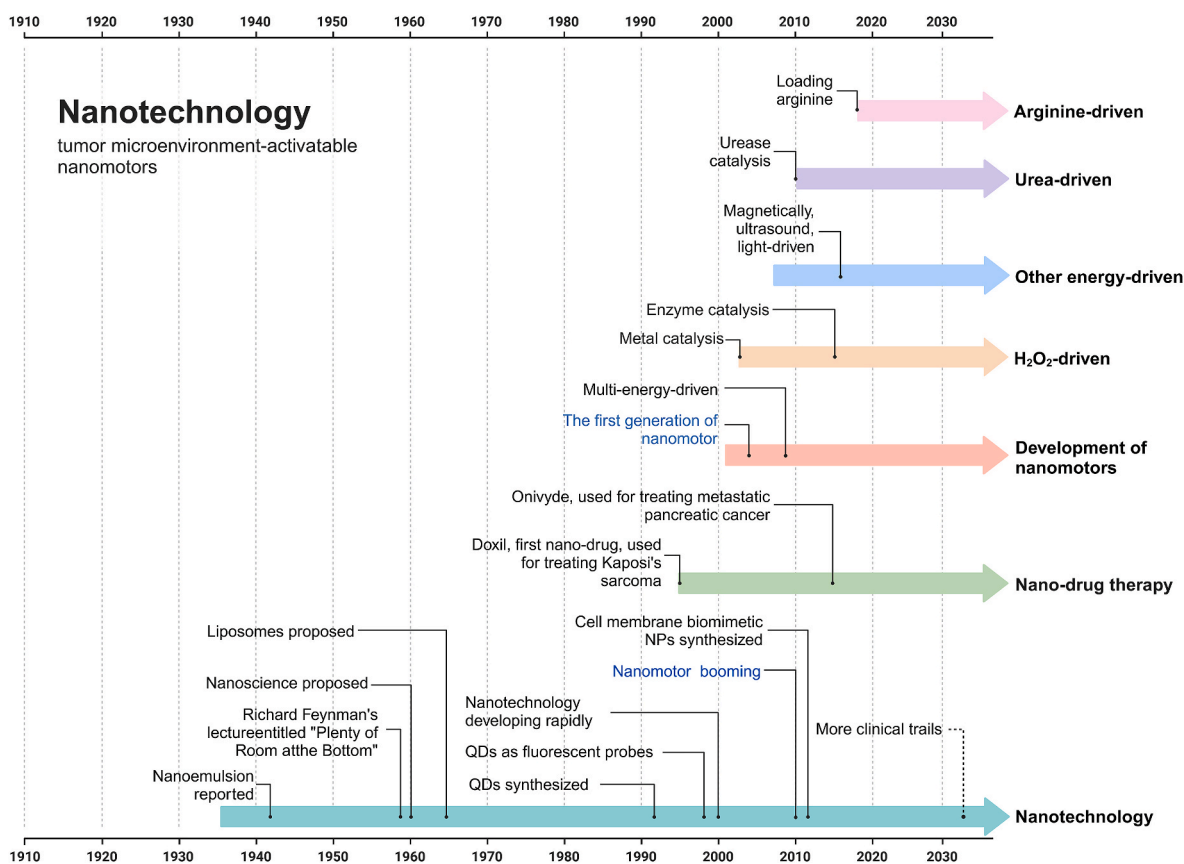


Fig. 1. Timeline of discoveries and research on nanotechnology and tumor microenvironment-activated nanomotors. Milestone discoveries are highlighted. Nanotechnology research began in the 1960s. In the ensuing 40 years, nanotechnology has flourished, giving rise to the emergence of nanomotor technology [41,45–59].

[75], a strategy involving continuous luminescence (PL) excitation PTT, synchronous thermotactic propulsion, and PL-triggered NO release was proposed, utilizing the continuous motion of ultrasound-activated nanoparticles to enhance cellular uptake, increase persistent PTT, and intracellular NO levels, thereby combating tumor cells without the use of any chemotherapy drugs. The continuous motion activated by ultrasound promotes the intratumoral accumulation and distribution of PTT/NO therapeutic drugs. Xing's research team [77] designed mesoporous carbon nanomotors coordinated with single-atom copper (Cu-JMCNs). It combines single-atom nano catalytic drugs with nano motion for cancer treatment. On one hand, single-atom Cu can utilize hydrogen peroxide to convert to toxic hydroxyl radicals (OH), used for chemodynamic therapy (CDT). On the other hand, carbon has an asymmetric structure and photothermal properties similar to jellyfish, and near-infrared light-triggered Cu-JMCNs achieve self-heating swimming motion, significantly enhancing the uptake and penetration of three-dimensional tumor cells. In vivo experiments have shown that the combined application of single-atom Cu for CDT and near-infrared light propulsion can achieve a tumor suppression rate of over 85 %.

Although targeted magnetic nanomotor drug delivery systems have advantages such as high magnetic field strength, long propulsion time, and accurate delivery, it is difficult to set precise gradients and rotate magnetic fields. This not only results in low drug loading efficiency but also necessitates further consideration of the long-term adverse effects caused by metals [78]. Compared to magnetic delivery, ultrasound can provide strong external driving force for targeted nanodrugs, allowing them to penetrate cells quickly and effectively. However, it suffers from drawbacks such as poor directional migration rates [79], low portability of equipment, and high operational difficulty [80]. The so-called light-driven nanomotor drug delivery system usually achieves control over the propulsion of nanomotors by controlling the magnitude of light energy (determined by wavelength or frequency) and the angle of incidence, leading to thermal effects or chemical reactions in different directions. These effects significantly affect the speed and direction of light-driven nanomotor drug delivery systems [81]. However, due to the weak penetration power of light, the application of these systems in cancer treatment is still limited (see Table 1).

The significant gap between current capabilities and the vision of efficient treatment prompts us to reflect soberly on the current status and future of research on targeted nanodrug delivery systems. In view of this demand, we seek to draw lessons from comparing various fundamental and practical issues of different types of nanomotors. In particular, we focus on a class of endogenous nanomotors, which can help us understand the working mechanisms and potential applications of nanomotors.

Endogenous nanomotor drug delivery systems aim to obtain energy from the tumor microenvironment or self-carried fuels through chemical reactions [82] or enzyme-catalyzed reactions [83], converting chemical energy into mechanical energy for self-propulsion. Compared to the aforementioned biologically hybrid or exogenous nanomotors, endogenous motors have unparalleled advantages. Firstly, endogenous

nanomotors do not require specific storage and usage conditions and can operate stably at room temperature and pressure. Secondly, these motors can generate driving forces through chemical reactions, enhancing the reliability and stability of the system (see Table 2).

#### 4.1. $H_2O_2$ -fueled nanomotors

Gas therapy based on gas molecules is a new approach to promoting synergistic treatment with other cancer therapies. Studies have shown that the release of sulfur dioxide gas can induce strong oxidative stress leading to depletion of glutathione (GSH) within cancer stem cells (CSC), further inhibiting CSC growth [116]. Yue's team [84] designed Au@MnO<sub>2</sub> gold nanoparticles loaded with sulfur dioxide (SO<sub>2</sub>) prodrug benzothiazole sulfinate (BTS) for catalytic decomposition of H<sub>2</sub>O<sub>2</sub> into oxygen bubbles by manganese dioxide, continuously powering the nanomotors to penetrate deep-seated solid tumors (Fig. 2A). SO<sub>2</sub> is selectively released in acidic environments to enhance the efficacy of gas therapy for cancer treatment.

One of the key criteria for evaluating nanomotors is the controlled release of drugs in vivo [117]. The impact of different motor speeds on drug release varies, making it necessary to explore methods for adaptively controlling nanomotor motion in response to environmental changes. To address this issue, Song et al. [86] investigated a pH-rate-regulated catalase-driven porous MOFtor (Fig. 2B). They assembled a binary composite superstructure of  $\beta$ -lactoglobulin and catalase (CAT) with permeability at neutral pH into porous framework particles (zeolitic imidazolate framework-L, ZIF-L). Under different pH conditions,  $\beta$ -lactoglobulin undergoes reversible gelation, controlling the entry of H<sub>2</sub>O<sub>2</sub> and resulting in different speeds and corresponding controlled release rates. Additionally, the porous framework enhances the biocatalytic activity of catalase, enabling it to utilize ultra-low concentrations of H<sub>2</sub>O<sub>2</sub> under physiological conditions. This nanosystem, utilizing both pH and chemical potential, may serve as a stimulus-responsive drug delivery carrier, potentially operating in complex biological environments.

Using ultrasound-assisted synthesis and wet chemistry, Wang et al. [87] prepared a micro-electric motor called MOF-NZ in the form of ZIF-67 framework (Fig. 3A). This micro-motor efficiently loads iron oxide NPs (nanoparticles) and fluorescent anticancer drug doxorubicin (DOX) (doxorubicin hydrochloride). Moreover, due to its degradability in water, this micro-motor exhibits high biocompatibility suitable for biomedical applications. The presence of numerous cavity structures in its framework enables rapid transfer of H<sub>2</sub>O<sub>2</sub> molecules within it, providing a continuous power source for the micro-motor. Extending the motor's operation time to 90 min and adjusting the speed adaptively based on H<sub>2</sub>O<sub>2</sub> concentration within the range of 15.3–76.3  $\mu$ m/s.

Although such nanomotors have the characteristics of rapidly generating bubbles and strong power, they behave like deflated balloons, only capable of completely random motion, with a high probability of failing to target the interior of tumors. In response to this, Zhang et al. [88] loaded magnetic iron oxide nanoparticles (IONPs) into

**Table 1**  
Comparison of nanomotor drug delivery systems propelled by exogenous and biohybrid power.

Type	Power source	Material	Performance in motion/advantage	Safety/limitation	Ref
Exogenous power	Electric Fields	Au,TiO <sub>2</sub>	Under the influence of external forces, it exhibits excellent directional stability and robust motility.	The intensity of the electric field decreases rapidly with increasing distance from the power source.	[67]
	Magnetic Fields	Fe		The potential hazards of magnetic metals to the human body.	[68]
	Light	Fe <sub>3</sub> O <sub>4</sub> ,Cu <sub>9</sub> S <sub>8</sub>		Ultraviolet light is harmful.	[69]
	Thermal	PDA		It may potentially induce thermal damage to surrounding normal tissues.	[70]
Biohybrid power	Ultrasound	Perfluorooctyl Bromide		Ultrasound may induce cellular oxidative stress.	[71]
	Bacteria	–	Overcoming multidrug resistance.	May elicit an immune response.	[63]
	Macrophage	–	Targeting inflammatory tissues.	May elicit an immune response.	[64]
	Sperm	–	Targeted therapy for ovarian-related cancers.	The lifespan of sperm is relatively short.	[65]

**Table 2**  
Chemically propelled nanomotors with potential biomedical applications.

Fuel	Primary Constituent Materials	Catalytic way	Size	Speed	Fuel Concentration	Merits and demerits	Ref
H <sub>2</sub> O <sub>2</sub>	Au@MnO <sub>2</sub>	MnO <sub>2</sub>	191 nm	8 pixel/ frame	0.1 mM	Abundant fuel (H <sub>2</sub> O <sub>2</sub> ); Oxygen generation, alleviating hypoxia. Weak ability to identify tumor heterogeneity.	[84]
H <sub>2</sub> O <sub>2</sub>	MnO <sub>2</sub> , PEG-PDLLA	MnO <sub>2</sub>	300 μm	15–20 μm/s	5–50 mM		[85]
H <sub>2</sub> O <sub>2</sub>	CAT -β@ZIF	Catalase (CAT)	1 μm	0.65–0.81 μm <sup>2</sup> /s	0.3–3%		[86]
H <sub>2</sub> O <sub>2</sub>	ZIF-67/Fe <sub>3</sub> O <sub>4</sub> /DOX	Co <sup>2+</sup> and 2-Methylimidazole	5 μm	76.38 μm/s	10 %		[87]
H <sub>2</sub> O <sub>2</sub>	L-arginine, HPAM	Catalase	170 nm	0.5–4 μm/s	5–20 mM		[56]
H <sub>2</sub> O <sub>2</sub>	Fe <sub>2</sub> O <sub>3</sub> , PEG-b-PS	Iron oxide nanoparticles (IONPs)	342.9 nm	307 nm/s	200 μM		[88]
H <sub>2</sub> O <sub>2</sub>	Pt, PEG-b-PS	Pt	152 nm	23 μm/s	35 %		[89]
H <sub>2</sub> O <sub>2</sub>	Pt, PEG-b-PS	Pt	150 nm	8.97 μm/s	Tumor microenvironment		[90]
H <sub>2</sub> O <sub>2</sub>	Pt, PEG-b-PS PEG-b-PCL	Pt	30 nm	39 μm/s	4.98 mM		[91]
H <sub>2</sub> O <sub>2</sub>	CAT, PEG-b-PS	Catalase	500 nm	60 μm/s	111 mM		[92]
H <sub>2</sub> O <sub>2</sub>	CAT, GOx, CAuNCs@HA	Catalase	171.53 nm	25.25 μm/s	100 μM		[93]
H <sub>2</sub> O <sub>2</sub>	CREKA-Ce@PDA/ DOX NBs	CeO <sub>2</sub>	150 nm	9.5 μm/s	4.9 mM		[94]
H <sub>2</sub> O <sub>2</sub>	UCNPs@mSiO <sub>2</sub> - TAPP @Au-3-MPBA	Catalase	59.8 nm	1.727 μm <sup>2</sup> / s	50 mM		[95]
H <sub>2</sub> O <sub>2</sub>	JAuNR-Pt	Pt	108 nm	10.18 μm/s	200 μM		[96]
H <sub>2</sub> O <sub>2</sub>	Au@Pt	Pt	100 nm	43.85 ± 5.49 μm/s	10 mM		[97]
H <sub>2</sub> O <sub>2</sub>	Cu-JMCNs	Cu	356 ± 4 nm	5–11 μm <sup>2</sup> /s	Not provided		[77]
H <sub>2</sub> O <sub>2</sub>	JHP@Catalase	Catalase	521 nm	0.63 ± 0.03 μm <sup>2</sup> /s	2.5 wt%		[98]
Urea	MSNP-Ur/PEG-Ab	Urease	481 nm	1.2 μm <sup>2</sup> /s	50 mM	Strong targeting towards regions with higher urea levels (kidneys, prostate, bladder cancer). Poor applicability, not suitable for urea-free sites.	[99]
Urea	Ur-PDA NC	Urease	5 μm	10.67 μm/s	100 mM		[100]
Urea	UPJNMs, Ur- PEG- AuNP	Urease	90 μm	11.1 μm <sup>2</sup> /s	10 mM		[101]
Urea	LM@PDA@CF & Ur	Urease	348 nm	0.825 μm <sup>2</sup> / s	50 mM		[102]
Urea	LL-37@K7- Pol@MSNPs@Ur	Urease	1.87 μm	0.58 μm <sup>2</sup> /s	200 mM		[103]
Urea	HSiO <sub>2</sub> FA-Urease-I	Urease	Not provided	12 μm/s	25 mM		[104]
Urea	HSiO <sub>2</sub> FA-Urease-O	Urease	Not provided	11 μm/s	50 mM		[104]
Urea	JRs@ HAase@ Ur	Urease, hyaluronidase	93–260 nm	4–8 μm/s	5 mM		[105]
Urea	JHP@Urease	Urease	495 nm	0.96 ± 0.04 μm <sup>2</sup> /s	300 mM		[98]
Urea	UM - NEs	Urease	254 nm	4.7 μm/s	50 mM		[106]
Arginine	L-arginine, HPAM	NO synthase (NOS), Reactive oxygen species (ROS)	385 nm	13 μm/s	3.75 mg/mL	Nitric oxide production; improving tumor microenvironment. Low sustained efficacy, limited fuel capacity (arginine); Reliant on tumor nitric oxide synthase.	[56]
Arginine	HFLA-DOX	NOS, ROS	50 nm	13.3 μm <sup>2</sup> /s	10 %		[107]
Arginine	HFCA	NOS, ROS	40 nm	10 μm <sup>2</sup> /s	Not provided		[108]
Arginine	PCBMA - LA	NOS, ROS	220 nm	3.5 μm/s	15 %		[109]
Arginine	PMA-TPP/PTX	NOS, ROS	200 nm	3 μm/s	Not provided		[110]
Arginine	DPNMs, L-Arg, CaO <sub>2</sub>	NOS, ROS	361 nm	6 μm/s	2.7 mM		[111]
Arginine	PCBMA-LA	NOS, ROS	220 nm	1.8 μm/s	121.7 μg/mL	[109]	
Arginine	TAP nanomotors	NOS, ROS	200 nm	5 μm/s	Not provided	[112]	
Glucose	AG-DMSNs, L-Arg AuNPs	gold nanoparticles (AuNPs) dendritic mesoporous silica nanoparticles (AG-DMSNs), H <sub>2</sub> O <sub>2</sub>	80 nm	11 μm/s	27.8 mM	Primary energy source for cells; Biocompatible fuel; Abundant in biological systems. Multiple conversion steps; Less efficient compared to direct chemical fuels.	[113]
Glucose	SiO <sub>2</sub> @Au&PMO Janus	Glucose Catalase	350 nm	6.34 μm <sup>2</sup> /s	100 mM		[114]
Glucose	GC6@cPt ZIFs	Glucose Catalase	70–120 nm	2.08 μm/s	10 × 10 <sup>-3</sup> M		[115]

self-assembled vesicle structures of PEG-b-PS, along with a photosensitizer, harnessing the advantage of external magnetic tropism, enabling the targeted delivery system of nanomotors to move directionally towards and aggregate near tumor tissues (Fig. 2C), thereby expanding the distribution of ZnPc, enhancing the reactive distribution of ROS, and boosting the activity of photodynamic therapy (PDT).

Polymer vesicles, a novel type of artificial vesicle, are composed of amphiphilic block copolymers. These vesicles can be transformed into

oral cells through dialysis-driven artificial endocytosis. Oral cells are nearly closed bowl-shaped polymer entities capable of trapping catalysts within their nanocavities, serving as self-propelled nanomotors. Wilson et al. [89] demonstrated for the first time a method to selectively capture catalytically active platinum nanoparticles within their nanocavities and subsequently use catalysis as the driving force for the autonomous motion of polymer oral cells. PtNPs were prepared using poly(ethylene glycol)-b-polystyrene (PEG-b-PS) as the material, selectively

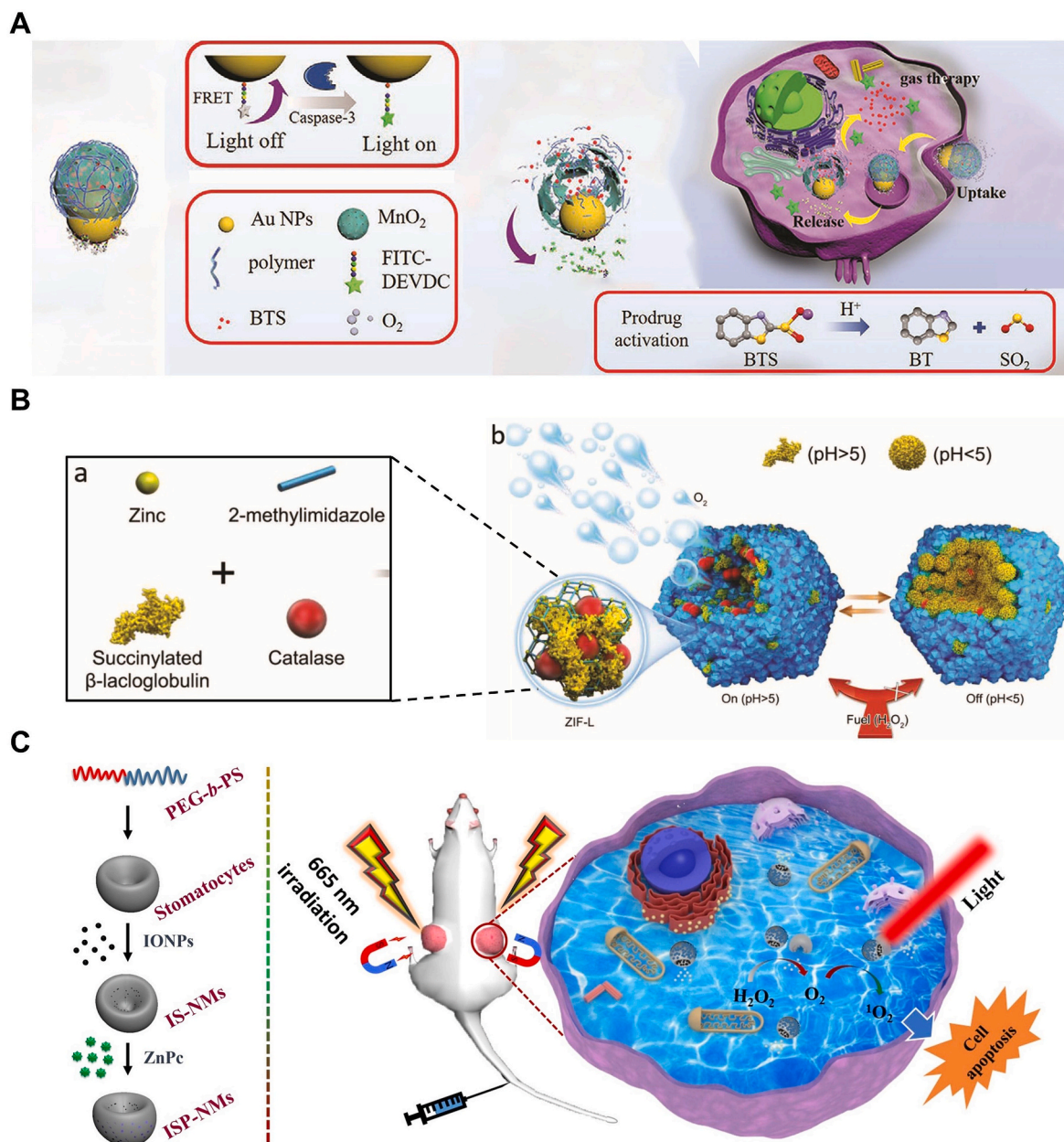


**Fig. 2.** Nanomotor systems propelled by H<sub>2</sub>O<sub>2</sub>. (A) Preparation of BTS-Au@MnO<sub>2</sub> nanomotors and self-reported gas therapy. Reproduced with permission [84]. Copyright 2021, John Wiley & Sons. (B) Schematic representation of the assembly of micromotors with pH-responsive on/off motion. Note the relative size between each component is not to scale. Reproduced with permission [86]. Copyright 2019, John Wiley & Sons. (C) Schematic diagram of magnetic field assistant tumor targeting of ISP-NMs and their <sup>1</sup>O<sub>2</sub> generation, movement and PDT process for cancer treatment. Reproduced with permission [88]. Copyright 2020, Elsevier.

encapsulating platinum nanoparticles within the nanocavities of polymer oral cells. Meanwhile, hydrogen peroxide can freely enter the interior of oral cells and be decomposed by the active catalyst (captured platinum nanoparticles) into oxygen and water, thereby causing thrust and directional motion.

However, achieving efficient, stable, and controllable operation of nanomotors in biological environments remains a challenge. To address this issue, the Abdelmohsen team proposed a strategy of enzyme capture and nanomotor assembly [92]. The core of this strategy is to fold polymer micelles into cavity cells under mild conditions, thereby achieving encapsulation of proteins (Fig. 3B). This method enables proteins to maintain their functionality and stability inside the cavities. Enzyme-driven nanomotors generated by this strategy exhibit high motility. They can propel these structures at low H<sub>2</sub>O<sub>2</sub> concentrations,

achieving autonomous motion in biological environments. Importantly, the confinement of enzymes inside the cavities does not hinder their activity; instead, it promotes substrate transfer. This is because the confined space inside the cavity facilitates interactions between enzymes and substrates, thereby enhancing catalytic efficiency. Meanwhile, enzymes are protected inside the cavities, shielded from deactivation by other components in the culture medium.

Although the miniaturization and motility of artificial nanomotors make them popular tools for exploring new and innovative biomedical cancer treatment strategies, integrating multiple functions on small moving entities is crucial for further therapeutic advancements. Represented by Chen's team [95], a dual-driven Janus nanomotor is introduced, consisting of a gold layer with up conversion nanoparticles (UCNPs) and mesoporous silica (mSiO<sub>2</sub>) core-shell structures, modified

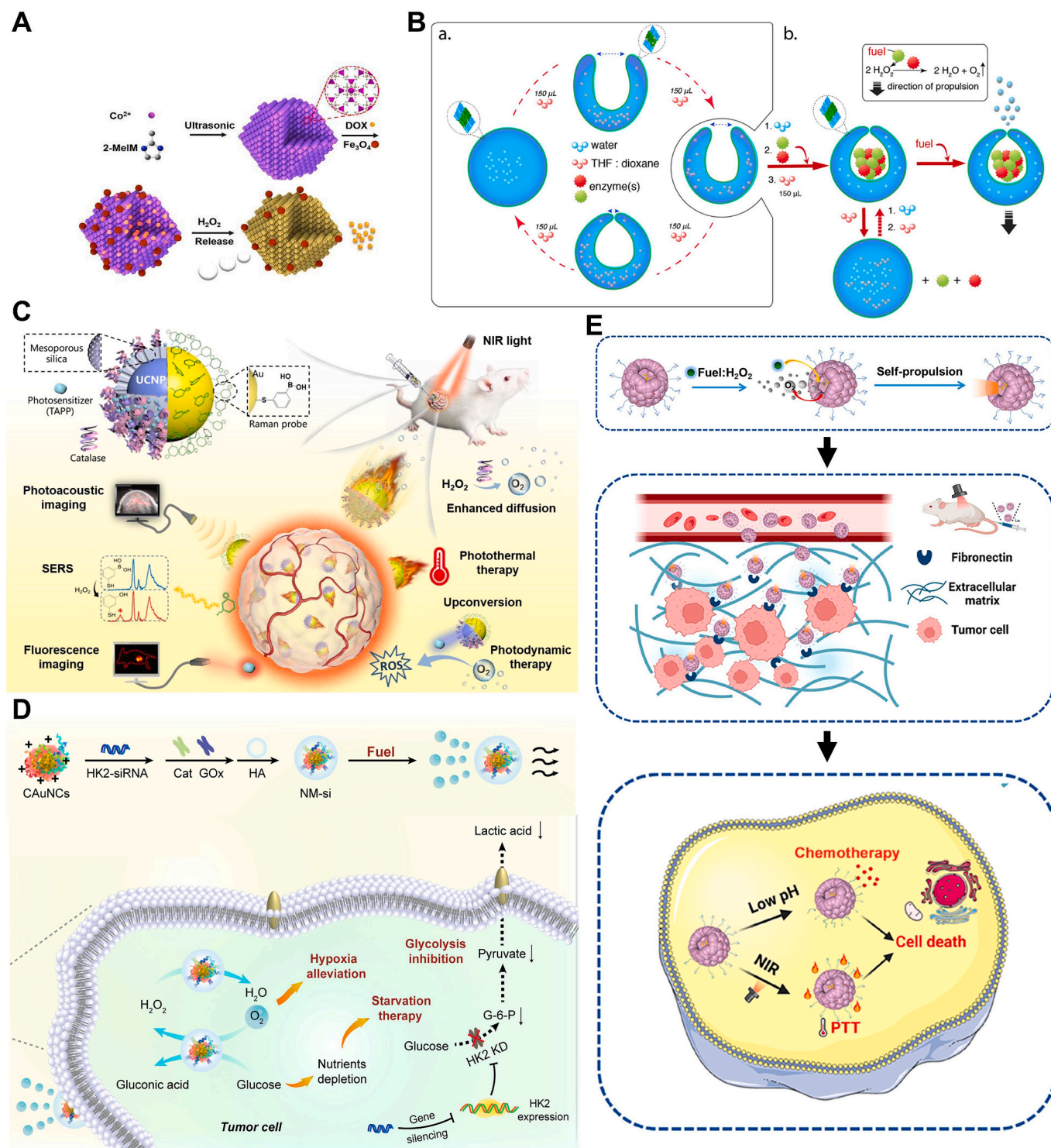


**Fig. 3.** Nanomotor systems propelled by H<sub>2</sub>O<sub>2</sub>. (A) Schematic illustration showing the processes of ZIF-67 micromotors, ZIF67/Fe<sub>3</sub>O<sub>4</sub>/DOX multifunctional micromotors fabrication and the mechanism of drug delivery. Reproduced with permission [87]. Copyright 2018, Royal Society of Chemistry. (B) Supramolecular assembly of the enzyme-driven nanomotor. Reproduced with permission [92]. Copyright 2016, American Chemical Society. (C) Schematic illustrating the dual-source powered nanomotor for SERS biosensing and multimodal cancer photo-theranostics. Reproduced with permission [95]. Copyright 2022, Elsevier. (D) Schematic illustration of the cascade enzyme-powered nanomotor (NM-si) for TME modulation. Reproduced with permission [93]. Copyright 2021, Elsevier. (E) Schematic illustration of the Preparation of CREKA-Modified Ceria@Polydopamine Nanobowls (CREKA-Ce@PDA NBs) and Their Application for Enhanced Tumor Penetration and Antitumor Effect. Reproduced with permission [94]. Copyright 2023, American Chemical Society.

with H<sub>2</sub>O<sub>2</sub>-sensitive 3-mercaptopropionic acid (3-MPBA) and photosensitizer 4-aminobenzyl phthalocyanine (TAPP). By modifying peroxidase and/or adding H<sub>2</sub>O<sub>2</sub> and using NIR laser at 808 nm, its penetration depth can be significantly increased (Fig. 3C). This demonstrates its

potential application in tumor diagnosis and treatment. The diffusion behavior of nanomotors in tumor spheroid models is enhanced, providing strong support for future research and applications.

Solid tumors commonly exhibit a significant characteristic - local hypoxia, leading to their high metastatic potential and insensitivity to chemotherapy. Compared to directly killing tumor cells, indirectly inhibiting tumor growth by reconstructing the tumor microenvironment is considered a novel approach. Therefore, providing sufficient oxygen to the root of the tumor and alleviating the Warburg effect [118] become key steps in implementing this therapeutic strategy. Based on this, Yu et al. [93] constructed a cascade enzyme-driven nanomotor (NM-si), consisting of glucose oxidase (GOx) and catalase (CAT), where GOx catalyzed the production of  $H_2O_2$  as a premise, and CAT continuously catalyzed the release of oxygen bubbles as a power source, allowing the entire delivery system to progress along the  $H_2O_2$  gradient between the bloodstream and the site of tumor occurrence (Fig. 3D). Meanwhile, during the enzyme-catalyzed reaction process, the continuously generated oxygen bubbles can alleviate the tumor hypoxia problem, ultimately achieving a “double hit” of delivery and oxygenation.

Addressing the issues of by-products and insufficient power in conventional nanomotors, Zhu's team [94] proposed a nanomotor composed of cysteine-arginine-glutamic acid-lysine-alanine (CREKA) asymmetrically modified cerium oxide@polydopamine nano-bowls (Fig. 3E), which continuously converts  $H_2O_2$  into propulsion for nanomotor advancement by leveraging the excellent redox cycling capability between  $Ce^{3+}$  and  $Ce^{4+}$ , while also avoiding the consumption of metal materials and by-products. Additionally, utilizing the force of receptor-ligand interaction, the tumor homing ligand CREKA specifically binds to the tumor integrin terminal fibronectin to achieve directional control of the nanomotor, ultimately achieving deep penetration. Loaded with the anti-tumor drug doxorubicin (DOX), optimal therapeutic effects are achieved through the “last step” of chemotherapy. Under 808 nm near-infrared (NIR) laser, the nanomotor rapidly depletes tumor microenvironment-specific hydrogen peroxide ( $H_2O_2$ ) in the nano-bowl, aiding in self-generated gradients, achieving rapid propulsion (9.5  $\mu\text{m/s}$  at 46 °C), and achieving deep penetration (70  $\mu\text{m}$  in multicellular spheroids), fulfilling the mission of deep tumor penetration, photothermal therapy, and chemotherapy drug release “triple therapy”.

#### 4.2. Urea -fueled nanomotors

Urea concentration is relatively high in the bladder, enabling urease-driven nanomotors to be utilized for the treatment of bladder cancer. By encapsulating therapeutic drugs within nanomotors, upon entry into the bladder, urease catalyzes the decomposition of urea into ammonia and carbon dioxide, generating energy to propel the nanomotors, thereby delivering drugs accurately to bladder cancer cells. This approach not only enhances the therapeutic efficacy of drugs but also reduces damage to normal tissues.

Bladder instillation therapy involves the introduction of drugs into the bladder via a catheter, retaining them for a certain period before voiding, to treat various bladder conditions such as cystitis and bladder cancer. As a localized treatment method, bladder instillation therapy offers the advantage of low toxicity as it solely affects the bladder mucosa without entering the bloodstream. However, this treatment method also faces challenging obstacles that need to be overcome urgently. Firstly, the bladder wall is coated with a mucosal layer composed of glycosaminoglycans (GAG), making efficient drug delivery challenging [119]. Additionally, regular urination flushes away the therapeutic drugs introduced into the bladder, necessitating frequent repeated injections to achieve the desired therapeutic effect [120]. Therefore, such an environment imposes high demands on the efficient adhesion, retention, and biocompatibility of the delivered drugs on the bladder wall.

In light of this, Choi's team [100] reported on nanomotors capable of deeply penetrating the mucosal layer of the bladder wall and remaining in the bladder for an extended period. Exploiting the high urea content in the existing environment, they surface-functionalized polydopamine

nano capsules (PDA NC) with urease (Fig. 4A). Experimental results demonstrated that upon the addition of urea (50 and 100 mM), these nanomotors exhibited rapid movement and significant directionality, achieving speeds of 4.56 and 10.67  $\mu\text{m/s}$ , respectively, and enhancing the maximum bladder wall penetration depth to 60  $\mu\text{m}$ .

Although bladder cancer can be treated through surgical means such as urinary tract resection, subsequent treatments for patients still rely on the assistance of immunotherapy or chemotherapy drugs, which also come with certain side effects. Therefore, frequent bladder endoscopy monitoring and retreatment of patients are required, making bladder cancer one of the most expensive cancers. Cristina et al. [121] innovatively addressed this issue by using radiolabeled  $^{131}\text{I}$  nanorobots for radioisotope therapy (Fig. 4B). These nanorobots are composed of mesoporous silica nanoparticles (MSNPs) with a diameter of approximately 450 nm, surface-modified with urease, polyethylene glycol, and gold nanoparticles, enabling self-propulsion in urine and accumulation and penetration into tumors. In a mouse model, these nanorobots were shown to effectively accumulate at tumor sites, confirmed by positron emission tomography scans. Additionally, observation under confocal microscopy of cleared bladder tissues confirmed the penetration of nanorobots into tumor tissues. Finally, radiotherapy administered to mice carrying tumors showed a reduction in tumor size by approximately 90 %, demonstrating the potential of nanorobots as an effective delivery system for bladder cancer therapy. This study provides new insights and methods for the treatment of bladder cancer.

Although urease-driven nanomotors can penetrate deep into cancer tissues, they still cannot address the issues of cancer cell proliferation and migration. Based on this, Samuel et al. [99] proposed a urease (Ur)-driven nanomotor based on mesoporous silica nanoparticles (MSNPs), with the outer surface containing polyethylene glycol and anti-FGFR3 antibody, which can target bladder cancer cells in the form of three-dimensional spheres (Fig. 4D). This autonomous movement is promoted by the inherent high concentration of urea in the bladder. Fibroblast growth factor receptor 3 (FGFR3), which is overexpressed in bladder cancer cells, was selected as the target for the antibody. The anti-FGFR3 antibody can bind to FGFR3 on the surface of bladder cancer cells, thereby disrupting their signaling pathways, inhibiting cell proliferation and migration. The modified nanomotors can swim in water and exhibit enhanced diffusion behavior dependent on the matrix. This means that in simulated or real urine, nanomotors can better interact with the surface of bladder cancer cells, increasing the chances of antibody-antigen binding, thereby reducing cell migration and proliferation and inhibiting the occurrence of malignant tumors. This targeted treatment approach based on nanomotors holds promise as an effective cancer therapy strategy and demonstrates potential in clinical applications.

Xu et al. [102] proposed urease-driven liquid metal (LM) nanomotors with multiple therapeutic functions and imaging signal capabilities. These nanomotors are based on Ga-In-Sn liquid alloy and serve as a trackable active nanoplatform by carrying urease-loaded nanorobots, combining therapeutic and potential diagnostic functions (Fig. 4C). The significance of this study lies in providing a new approach for designing and constructing self-propelled nanomotor carriers. In addition to possessing self-propulsion capabilities, this motor carrier also exhibits various therapeutic and potential diagnostic functions. Successful tracking and monitoring of motor carrier movement were achieved through bimodal imaging of ultrasound and photoacoustic properties, serving the purpose of dynamic imaging.

Enzyme-catalyzed nanomotors have shown great potential in biological separation and sensing imaging due to their excellent biocompatibility, high turnover rate, and ease of access. However, the flow fields generated by enzyme-catalyzed reactions may affect the interaction between targets and ligands (or antibodies) due to inherent spatial conflicts, especially for recognition units (such as ligands) and target binding on MNMs. Therefore, to ensure the effective operation of sensing systems, it is crucial to distribute functional modules (antibodies



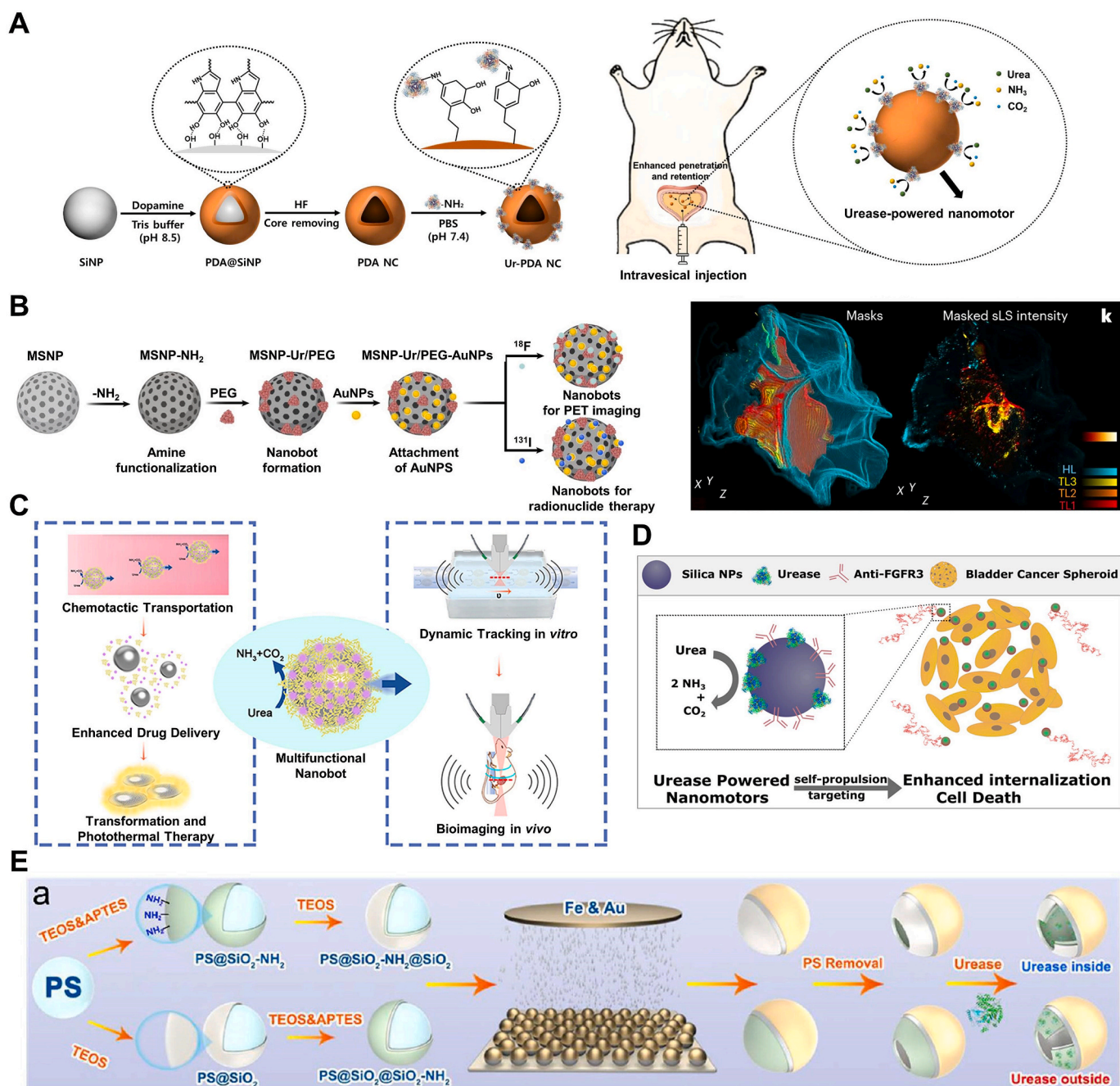


**Fig. 4.** Nanomotor systems propelled by urea. (A) Schematic illustration for the intravesical delivery of urease-powered nanomotors to enhance penetration and retention in the bladder and the preparation procedure of urease (Ur) powered nanomotors using silica nanoparticle (SiNP) and polydopamine nanocapsule (PDA NC). Reproduced with permission [100]. Copyright 2020, American Chemical Society. (B) Schematic illustration of urease-driven urease robots targeting bladder cancer with radionuclides. Reproduced with permission [121]. Copyright 2020, Springer Nature. (C) Schematic diagram of enzyme-driven liquid metal nanorobots with dual-mode photoacoustic and ultrasound imaging for synergistic photothermal and chemotherapy antibacterial therapy. Reproduced with permission [102]. Copyright 2021, American Chemical Society. (D) Schematic diagram of a urease-driven nanomotor of mesoporous silica nanoparticles with polyethylene glycol and anti-FGFR3 antibody on the outer surface. Reproduced with permission [99]. Copyright 2018, American Chemical Society. (E) Preparation and characterization of HSiO<sub>2</sub> FA-Urease-I (Urease inside) and HSiO<sub>2</sub> FA-Urease-O (Urease outside) micromotors. (a) Schematic diagram depicting the experimental process employed to fabricate HSiO<sub>2</sub>FA-Urease-I and HSiO<sub>2</sub>FA-Urease-O micromotors. Reproduced with permission [104]. Copyright 2021, American Chemical Society.

or ligands) and motor modules (enzymes) at different positions of MNMs [104]. In this regard, Liu et al. developed a selectively enzyme-localized urease micromotor for capturing and sensing exosomes. To achieve controlled distribution of enzymes, amino groups were selectively attached to the inner/outer surfaces of hollow SiO<sub>2</sub> using a two-step co-condensation method, and urease was finally fixed in the hollow structure with amino group modification by glutaraldehyde

cross-linking, resulting in HSiO<sub>2</sub>FA-Urease-I micromotors with urease located inside and HSiO<sub>2</sub>FA-Urease-O micromotors with urease located on the outer layer of SiO<sub>2</sub> (Fig. 4E). Through evaluation of their motility performance, the critical role of modified enzyme position in determining the distribution of generated flow fields was revealed. This study enables a better understanding of the role and impact of enzymes in MNMs, which will facilitate the development of more efficient, stable,

and reliable MNM devices, laying a solid foundation for their future practical applications.

Endogenous urea-powered urease-driven nanomotors, when injected into the bladder, demonstrate uniform distribution and enhanced fluid mixing [122], enabling imaging tracking, drug delivery, and targeted therapy of bladder tumors [123]. The active collective dynamic behavior, coupled with medical imaging tracking, constitutes an important milestone and progress in the field of biomedical nanorobots. Additionally, neutrophils with urease-driven motors have been shown to target thrombi and promote thrombolysis by releasing urokinase's thrombolytic protein drugs at thrombus sites [106], further enriching the diversity of urease-powered nanomotor motion system functions, expanding the application areas and therapeutic targets of nanomotors.

#### 4.3. Arginine -fueled nanomotors

With the innovation of biomedical discoveries and technological advancements, gas-mediated therapy has attracted widespread attention due to its high therapeutic efficacy and biocompatibility [124]. Nitric

oxide (NO) released from currently clinically used nitrite donors serves as an example, demonstrating its effectiveness in treating conditions such as angina and heart failure. Nowadays, numerous studies are dedicated to exploring the potential therapeutic applications of NO, particularly in the field of cancer treatment [125].

By the on-demand release of NO in the tumor microenvironment (TME), not only can the expression of mammalian HIF-1 $\alpha$ , base excision DNA repair enzyme, and multidrug transporter protein P-glycoprotein (P-gp) be inhibited, but tumor vasculature normalization can also be achieved, greatly enhancing the therapeutic effects of tumors [126]. NO not only exhibits direct cytotoxic effects on cancer cells but also enhances the efficacy of various treatment modalities [127]. Furthermore, it is worth noting that due to the extremely short half-life of NO (less than 5 s), the delivery of NO must be highly targeted and selective [128]. Therefore, NO-driven nano-targeted delivery systems have become a hot topic in cancer treatment in recent years. At the intersection of NO-based diagnosis and therapy integration and biomedical nanotechnology, NO-driven nanomotors have also made remarkable progress in cancer diagnosis and treatment.

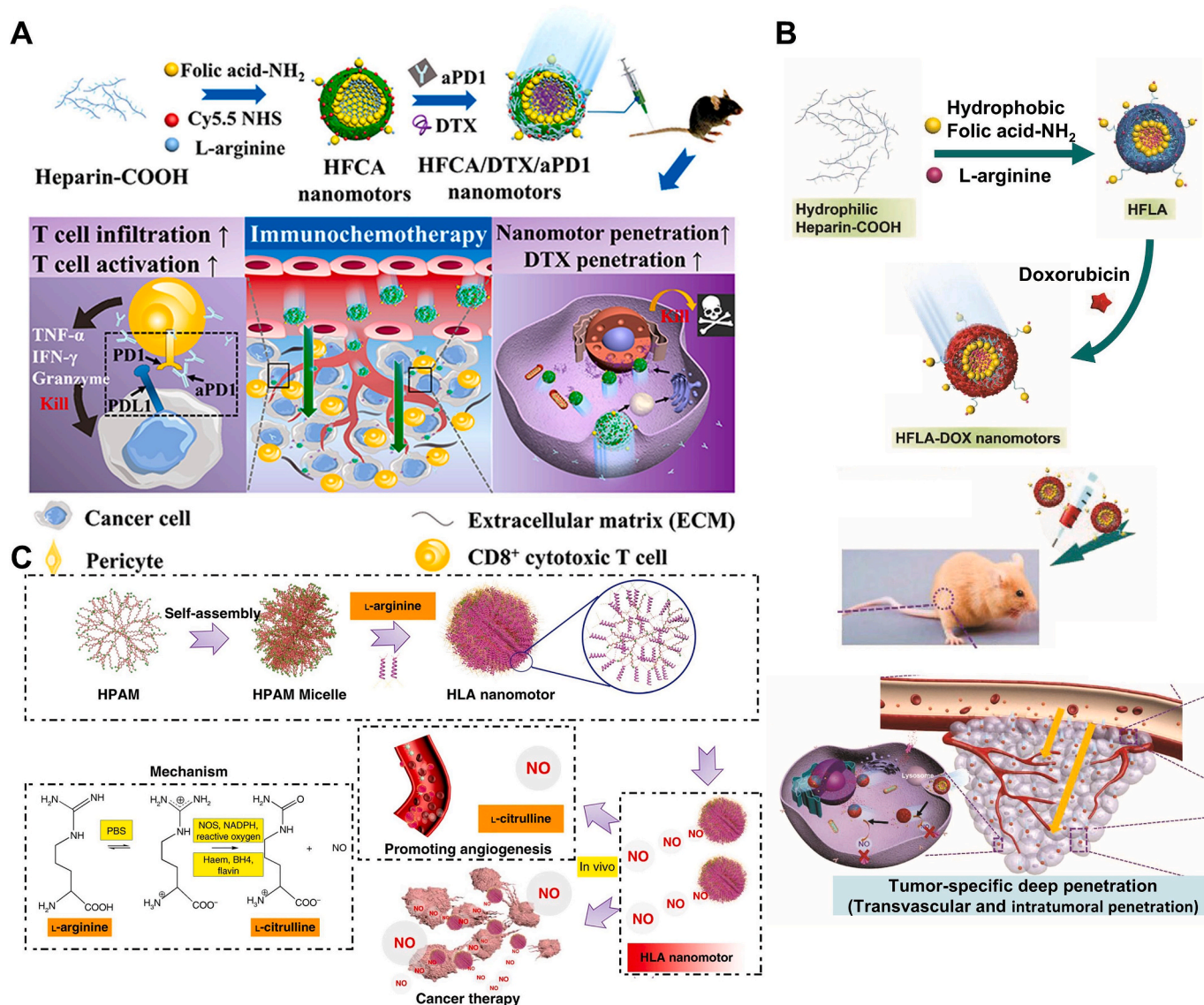


**Fig. 5.** Nanomotor systems propelled by arginine. (A) Synthetic Route of HFCA/DTX/aPD1 Nanomotor and the Schematic Illustration of Regulatory Mechanism of Combined Immunotherapy and Chemotherapy. Reproduced with permission [108]. Copyright 2021, American Chemical Society. (B) The fabrication process of HFLA-DOX nanomotors and the versatility of NO. Reproduced with permission [107]. Copyright 2020, John Wiley & Sons. (C) Schematic illustration of the formation of zwitterion-based nanomotor and the NO generation principle. Reproduced with permission [56]. Copyright 2019, Springer Nature.

In the healthy human body, NO is produced through the enzymatic reaction of endogenous L-arginine (L-Arg) with nitric oxide synthase (NOS), primarily expressed in the endothelium and neurons of brain tissue in isoforms (eNOS, nNOS) [129]. However, tumor cells also contain abundant nitric oxide synthase (NOS) [130], providing excellent conditions for the nano-motor drug delivery system to catalyze the release of NO bubbles by enzyme reaction with L-arginine, facilitating the dual penetration of nano-systems into tumor cells and tissues. Wang et al. [107] proposed a NO-driven nanomotor strategy using cage-like structured heparin and folate (HF) composite nanoparticles as carriers, loaded with L-arginine and doxorubicin (DOX) (Fig. 5B). With the active targeting of HF and enzyme-catalyzed reaction, the released NO bubbles drive the nano-targeted drug delivery system to penetrate into the interior of tumor cells. While releasing NO to improve the tumor microenvironment, it also reduces the expression of programmed cell death ligand 1 (PD-L1) on tumor cells, thereby exerting a synergistic therapeutic effect and enhancing the treatment efficacy.

Although there have been reports on nanomotors promoting the penetration of themselves and loaded drugs into tumor tissues, there is still a lack of relevant data on whether this motility effect can facilitate the deep infiltration of micrometer-scale immune cells into tumor tissues in their microenvironment. In-depth research on this issue is crucial for determining whether nanomotor technology can bring new breakthroughs in immunotherapy. Chen et al. [108] constructed a NO-driven nanomotor, named heparin-folate-cy5.5/L-arginine (HFCA), which promotes the normalization of tumor vasculature and degradation of extracellular matrix (ECM) by releasing NO, thereby significantly enhancing the infiltration capability of T cells into tumors in vivo (Fig. 5A). The infiltration efficiency of T cells in tumor tissues increased from 2.1 % to 28.2 %. The combination of the motility of this nanomotor power source and its physiological function provides more design ideas for the future immunotherapy of many diseases.

It is worth noting that common chemically fueled nanomotors (such as magnesium-based, platinum-based, and enzyme-based ones) produce certain by-products ( $H_2$ , ammonia,  $Mg(OH)_2$ , Pt) during their motion process, leading to toxic effects (e.g., excessive  $H_2$  may cause gas embolism) [131], which also hinders the clinical translation of these nanomotors. Therefore, designing a zero-waste, self-destructing nanomotor is of great significance. Wan et al. [56] reported a nanomotor synthesized from medical-grade fluorescent hyperbranched polyamide (HPAM) and biocompatible amphiphilic polymer L-arginine, termed hyperbranched polyamide/L-arginine (HLA) nanomotor. By simulating the action of nitric oxide synthase (NOS) and reactive oxygen species (ROS) in the human body, L-arginine is converted into NO, thereby achieving motility. The HPAM used in the experiment is synthesized from methyl acrylate and ethylenediamine monomers, which is almost not degraded in the human body (Fig. 5C), thus possessing excellent biocompatibility and stability. Additionally, due to its molecular weight being less than 1000, it can be naturally cleared from the body through glomerular filtration. Another advantage of HPAM is that its derived HLA nanomotor exhibits unique fluorescent properties, allowing monitoring of its entry into cells without the use of toxic dyes, which is expected to achieve in vivo tracking of nanomotors in the future.

## 5. Conclusion and outlook

Currently, nanomotor drug delivery systems for cancer treatment continue to encounter several challenges. such as the specific recognition and efficient elimination of tumor cells in vivo. Despite ongoing efforts by researchers to address these limitations, the ultimate “perfect” nanomotor has not yet been developed. Therefore, there is a necessity to explore more innovative active interaction modes, self-propelled traversal through dense network barriers, and achieve deep penetration into tumors.

The complex circulatory system and tumor microenvironment present significant challenges for nanomotors. Once introduced into the

bloodstream, they inevitably interact with biomolecules present in body fluids. Most nanocarriers are influenced by blood substances, leading to the formation of a “protein corona” on their surface. A prominent consequence of the protein corona (PC)-induced alteration in nanoparticle-cell interactions is the loss of the cellular targeting function of functional ligands [132]. Pioneering work by Anna et al. [133] revealed that when transferrin nanoparticles are exposed to a biological environment, proteins form a protein corona, masking the targeting molecules on the transferrin surface. This results in a loss of targeting specificity, posing a stringent challenge to achieving specific targeting with functionalized nanoparticles. Additionally, the PC impedes the interaction between the chemical reactants on the surface of nanomotors and the surrounding environment, thereby inhibiting catalytic reactions. This means that nanomotors cannot continue to generate movement or achieve their intended function [134,135].

Given the adverse effects of PC on the performance of nanoparticles, researchers are actively exploring and developing new strategies and materials to reduce protein corona formation, thereby enhancing the stability and targeting of nanoparticles in biological environments. One common approach is to achieve a “stealth” effect by grafting hydrophilic polymers such as polyethylene glycol (PEG) [136]. For instance, PEG-modified nanomotors can render the particle surface potential negative. Negatively charged nanomotors are more likely to repel similarly negatively charged proteins, reducing nonspecific protein adsorption and, consequently, the formation of a protein corona.

In addition, pre-coating nanomotors is a viable strategy. By interacting with biomembranes or surfactants, a controllable coating layer can form, mimicking the interactions between cells and the physiological environment, thereby reducing nonspecific protein adsorption. Yang et al. [137] proposed a strategy for constructing cancer vaccines by coating immunoadjuvant nanoparticles with mannose-modified cancer cell membranes. The cancer cell-coated nanoparticles can serve as tumor-specific antigens to stimulate anti-tumor immune responses and enhance the uptake by antigen-presenting cells, particularly promoting the maturation of dendritic cells, thereby triggering a strong anti-tumor immune response. Cao et al. [138], through CRISPR-Cas9 genome editing technology, identified ALOX15, a key gene driving ferroptosis, and encapsulated its saRNA in mesoporous polydopamine (MPDA). The assembly of saALOX15-loaded MPDA was then coated with modified macrophage membranes to avoid phagocytosis by the mononuclear phagocyte system (MPS), promoting the uptake of NPs by glioblastoma (GBM) and thereby enhancing ferroptosis in GBM cells. These efforts contribute to theoretical exploration and prospects for the targeted chemotaxis of nanomotors to deeper layers of tumors.

The speed of chemically driven nanomotors is not ideal [139], even if the catalytic reaction is highly efficient and fast, the speed generated within the nanomotor is still only tens of body lengths per second, while ultrasound-driven nanomotors can achieve high-speed motion, reaching up to 200  $\mu\text{m}$  per second, which is equivalent to covering 100 body lengths per second [140]. This means that they may not meet some of the high-speed and efficiency requirements in practical applications. On the one hand, their motion ability mainly depends on the rate and efficiency of chemical reactions. However, due to the special properties of the blood environment, such as high ion concentration, pH changes, and the presence of complex biomolecules, chemically driven nanomotors have relatively slow movement speeds in the blood. On the other hand, the design and size of nanomotors also affect their motion ability. Smaller nanomotors usually have higher speeds but face challenges in stability and controllability. Therefore, it is necessary to balance the relationship between size and motion ability when designing nanomotors.

Furthermore, the capacity for penetration exhibited by nanomotors is intricately linked to their respective fuel sources. The review has meticulously compiled a variety of fuel-driven nanomotors, systematically evaluating the advantages and limitations associated with each fuel type. As the saying goes, every coin has two sides. Therefore, the

selection of an appropriate fuel source is vital for deep tumor penetration.

Moreover, we expect nanorobots to possess the ability to rapidly respond to the tumor microenvironment, utilizing various chemical reactions to generate autonomous propulsion, enabling swift chemotaxis and internalization into tumor cells [141]. Additionally, the substances produced by these chemical reactions should also exhibit anti-tumor effects [142]. There are some fundamental strategies to consider. 1) Exploring ligand/membrane-coated nanomotors. The surface of the nanomotor could be modified with high-affinity biomolecules (such as peptides, small molecule ligands, antibodies, etc.). These biomolecules can bind to specific receptors on the surface of tumor cells, thereby facilitating the rapid internalization of the nanomotor by the tumor cells or directing it towards deeper regions of the tumor. Additionally, coating with cell membranes (e.g., macrophage membranes [143], cancer cell membranes [144]) is an alternative strategy to circumvent the complex issues we have detailed above (such as the influence of the protein corona) while enhancing the interaction between the nanomotors and tumor cells, thereby improving therapeutic efficacy. To release the encapsulated nanomotors and initiate the chemical reaction, a method must be employed to remove the so-called “cell protective

layer.” This can be achieved by using photothermal perturbation of the cell membrane to accomplish this task (Fig. 6).

Indeed, while harnessing the robust propulsion of a rapidly advancing nanomotor, it is also essential to effectively utilize the products of enzymatic reactions. By coating or modifying the nanomotor with various catalysts or enzymes, it can not only enhance its propulsion efficiency but also trigger a series of beneficial reactions in specific environments. For instance, by producing gases such as hydrogen sulfide, carbon monoxide, sulfur dioxide, and other specific gases, the nanomotor can further induce apoptosis in tumor cells or disrupt the tumor microenvironment. This approach enhances the penetration ability and therapeutic efficacy of the nanomotor, ultimately inhibiting tumor growth and metastasis.

Currently, nanomotors primarily rely on chemical response elements such as urea, hydrogen peroxide, and arginine to respond to the tumor microenvironment. These elements can trigger the movement and functionality of nanomotors under specific chemical conditions within the tumor microenvironment. However, with an increasing understanding of the complexity of the tumor microenvironment, relying solely on these chemical response elements may not fully address the diverse requirements of different types and stages of tumors. The future

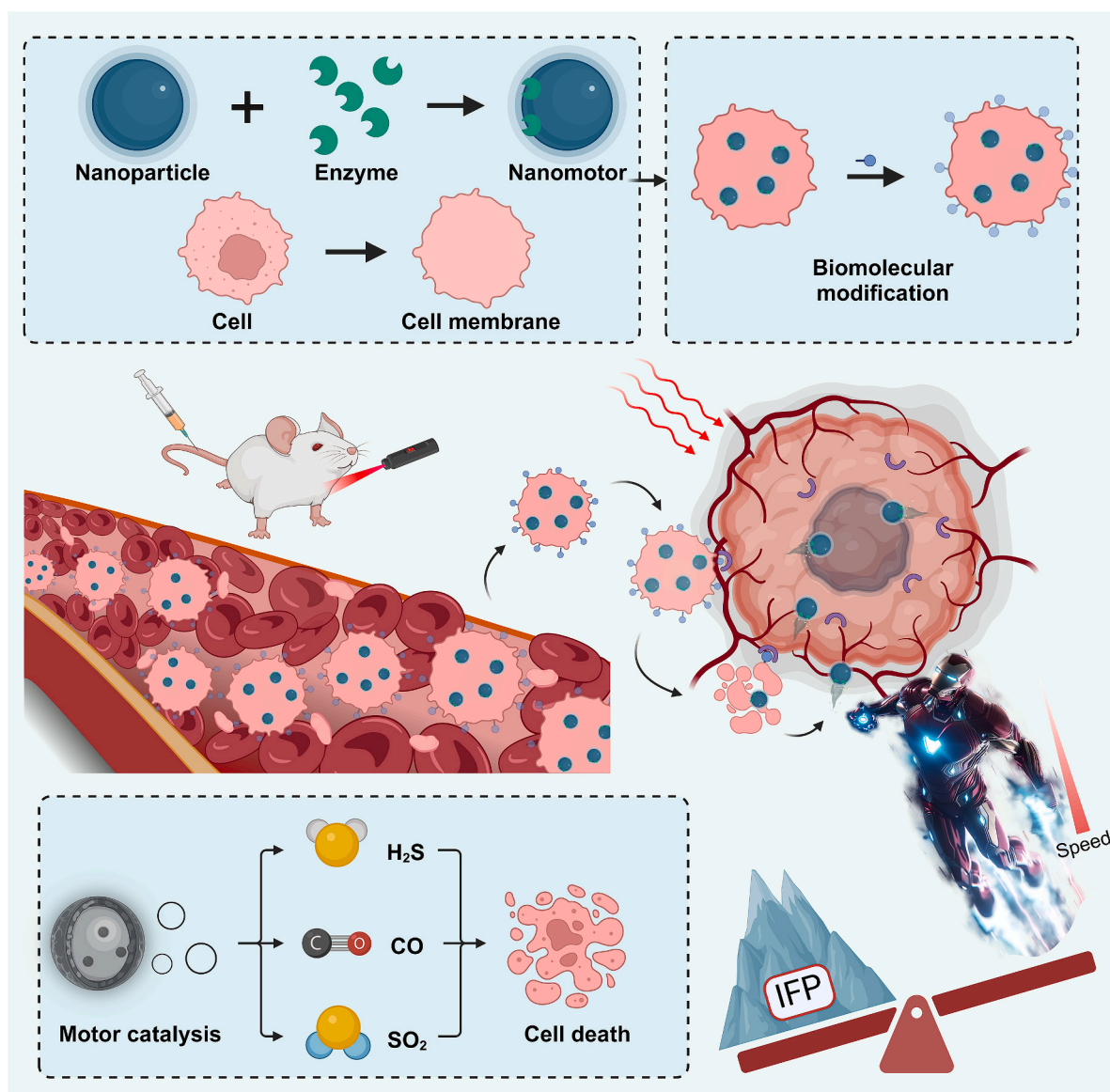


Fig. 6. Schematic illustration of precision targeting nanomotors for tumor cells.

development of nanomotors will inevitably involve the exploration of more diverse response sources. For instance, mechanically pressure-sensitive nanomotors will emerge as a crucial research direction. These nanomotors can respond to mechanical pressure changes in the tumor microenvironment, particularly as tumor growth progresses and the distribution of tumor interstitial pressure and surrounding pressure changes significantly. By utilizing this mechanical signal, nanomotors can more precisely locate and penetrate tumor tissues, thereby enhancing therapeutic efficacy.

Looking to the future, similar to the Apollo program that sent humans to the moon, dispatching “customized doctors” - “nanorobots” to treat cancer in the body is also an ambitious and challenging project. With the development of new materials and drug preparation technologies, nanomotor drug delivery systems are expected to precisely locate and attack cancer cells like “miniature submarines”, while avoiding damage to normal cells, bringing about revolutionary changes in human health and well-being.

### Funding

This study was supported by the National Natural Science Foundation of China (82372109).

### CRediT authorship contribution statement

**Qianyang Jiang:** Writing – original draft, Methodology, Investigation, Formal analysis, Data curation, Conceptualization. **Jiahuan He:** Investigation. **Hairui Zhang:** Writing – review & editing, Conceptualization. **Haorui Chi:** Investigation. **Yi Shi:** Software, Funding acquisition, Conceptualization. **Xiaoling Xu:** Writing – review & editing, Resources, Funding acquisition.

### Declaration of competing interest

The authors declare no competing interests.

### Data availability

No data was used for the research described in the article.

### References

- [1] R.S. Zheng, et al., Cancer incidence and mortality in China, 2016, *Journal of the National Cancer Center* 2 (2022) 1–9.
- [2] M. Yi, et al., Combination strategies with PD-1/PD-L1 blockade: current advances and future directions, *Mol. Cancer* 21 (2022) 28.
- [3] H. Qiu, S. Cao, R. Xu, Cancer incidence, mortality, and burden in China: a time-trend analysis and comparison with the United States and United Kingdom based on the global epidemiological data released in 2020, *Cancer Commun.* 41 (2021) 1037–1048.
- [4] W.A. Hall, et al., Magnetic resonance linear accelerator technology and adaptive radiation therapy: an overview for clinicians, *Ca-Cancer J. Clin.* 72 (2022) 34–56.
- [5] C.B. Falkson, et al., Surgical, radiation, and systemic treatments of patients with thymic epithelial tumors: a systematic review, *J. Thorac. Oncol.* 18 (2023) 299–312.
- [6] R.S. Riley, C.H. June, R. Langer, M.J. Mitchell, Delivery technologies for cancer immunotherapy, *Nat. Rev. Drug Discov.* 18 (2019) 175–196.
- [7] E.C. Scott, et al., Trends in the approval of cancer therapies by the FDA in the twenty-first century, *Nat. Rev. Drug Discov.* 22 (2023) 625–640.
- [8] S. Zinn, et al., Advances in antibody-based therapy in oncology, *Nat. Can. (Ott.)* 4 (2023) 165–180.
- [9] L. Kraehenbuehl, C.H. Weng, S. Eghbali, J.D. Wolchok, T. Merghoub, Enhancing immunotherapy in cancer by targeting emerging immunomodulatory pathways, *Nat. Rev. Clin. Oncol.* 19 (2022) 37–50.
- [10] W. Zeng, et al., Polypyrrole nanoenzymes as tumor microenvironment modulators to reprogram macrophage and potentiate immunotherapy, *Adv. Sci.* 9 (2022) e2201703.
- [11] Q. Li, et al., Symphony of nanomaterials and immunotherapy based on the cancer-immunity cycle, *Acta Pharm. Sin. B* 12 (2022) 107–134.
- [12] S. Taefehshok, et al., Cancer immunotherapy: challenges and limitations, *Pathol. Res. Pract.* 229 (2022).
- [13] E.C. Morris, S.S. Neelapu, T. Giavridis, M. Sadelain, Cytokine release syndrome and associated neurotoxicity in cancer immunotherapy, *Nat. Rev. Immunol.* 22 (2022) 85–96.
- [14] Z. Lu, et al., The landscape of cancer research and cancer care in China, *Nat. Med.* 29 (2023) 3022–3032.
- [15] X. Wang, X. Zhong, Z. Liu, L. Cheng, Recent progress of chemodynamic therapy-induced combination cancer therapy, *Nano Today* 35 (2020) 100946.
- [16] Z. Xiao, et al., State of the art advancements in sonodynamic therapy (SDT): metal-organic frameworks for SDT, *Chem. Eng. J.* 449 (2022) 137889.
- [17] S. Zhu, et al., Low-dose X-ray radiodynamic therapy solely based on gold nanoclusters for efficient treatment of deep hypoxic solid tumors combined with enhanced antitumor immune response, *Theranostics* 13 (2023) 1042–1058.
- [18] L. He, et al., Intelligent manganese dioxide nanocomposites induce tumor immunogenic cell death and remould tumor microenvironment, *Chem. Eng. J.* 461 (2023) 141369.
- [19] P. Zhao, H. Li, W. Bu, A forward vision for chemodynamic therapy: issues and opportunities, *Angew Chem. Int. Ed. Engl.* 62 (2023) e202210415.
- [20] L. Song, L. Lu, Y. Pu, H. Yin, K. Zhang, Nanomaterials-based tumor microenvironment modulation for magnifying sonodynamic therapy, *Acc. Mater. Res.* 3 (2022) 971–985.
- [21] Z. Xu, et al., Monte Carlo simulation-guided design of a thorium-based metal-organic framework for efficient radiotherapy-radiodynamic therapy, *Angew Chem. Int. Ed. Engl.* 61 (2022) e202208685.
- [22] Q. Yu, et al., Recent advances in reprogramming strategy of tumor microenvironment for rejuvenating photosensitizers-mediated photodynamic therapy, *Small* 20 (2024) e2305708.
- [23] S. Sheng, et al., An apoptotic body-based vehicle with navigation for photothermal-immunotherapy by precise delivery and tumor microenvironment regulation, *Adv. Funct. Mater.* 33 (2023) 2212118.
- [24] J. Wang, et al., Phage-Ce6-Manganese dioxide nanocomposite-mediated photodynamic, photothermal, and chemodynamic therapies to eliminate biofilms and improve wound healing, *ACS Appl. Mater. Interfaces* 15 (2023) 21904–21916.
- [25] G. Ma, et al., H(2) O(2) -responsive NIR-II AIE nanobomb for carbon monoxide boosting low-temperature photothermal therapy, *Angew Chem. Int. Ed. Engl.* 61 (2022) e202207213.
- [26] S.B. Aboelenen, M.A. Scully, J.C. Harris, E.H. Sterin, E.S. Day, Membrane-wrapped nanoparticles for photothermal cancer therapy, *Nano Converg* 9 (2022) 37.
- [27] Y. Du, et al., NIR-II fluorescence imaging-guided hepatocellular carcinoma treatment via IR-1061-acridine and lenvatinib co-loaded thermal-sensitive micelles and anti-PD-1 combinational therapy, *Chem. Eng. J.* 454 (2023).
- [28] X.L. Xu, et al., Nanodevices for deep cartilage penetration, *Acta Biomater.* 154 (2022) 23–48.
- [29] N. Meher, et al., Prostate-specific membrane antigen targeted deep tumor penetration of polymer nanocarriers, *ACS Appl. Mater. Interfaces* 14 (2022) 50569–50582.
- [30] R. Tong, D.S. Kohane, New strategies in cancer nanomedicine, *Annu. Rev. Pharmacol. Toxicol.* 56 (2016) 41–57.
- [31] G. Bazzoni, E. Dejana, Endothelial cell-to-cell junctions: molecular organization and role in vascular homeostasis, *Physiol. Rev.* 84 (2004) 869–901.
- [32] X. Yang, et al., Targeting endothelial tight junctions to predict and protect thoracic aortic aneurysm and dissection, *Eur. Heart J.* 44 (2023) 1248–1261.
- [33] J.C. García-Cañaveras, L. Chen, J.D. Rabinowitz, The tumor metabolic microenvironment: lessons from lactate, *Cancer Res.* 79 (2019) 3155–3162.
- [34] T.D. McKee, et al., Degradation of fibrillar collagen in a human melanoma xenograft improves the efficacy of an oncolytic herpes simplex virus vector, *Cancer Res.* 66 (2006) 2509–2513.
- [35] R.K. Jain, Delivery of molecular and cellular medicine to solid tumors, *Adv. Drug Deliv. Rev.* 64 (2012) 353–365.
- [36] P.Y. He, et al., Dual-stage irradiation of size-switchable albumin nanocluster for cascaded tumor enhanced penetration and photothermal therapy, *ACS Nano* (2022).
- [37] H. Li, et al., Medical micro- and nanomotors in the body, *Acta Pharm. Sin. B* 13 (2023) 517–541.
- [38] C. Wang, J. Xu, Y. Zhang, G. Nie, Emerging nanotechnological approaches to regulating tumor vasculature for cancer therapy, *J. Contr. Release* 362 (2023) 647–666.
- [39] Q. Li, et al., pH-labile artificial natural killer cells for overcoming tumor drug resistance, *J. Contr. Release* 352 (2022) 450–458.
- [40] Y. Hu, W. Liu, Y. Sun, Self-propelled micro-/nanomotors as “on-the-move” platforms: cleaners, sensors, and reactors, *Adv. Funct. Mater.* 32 (2021).
- [41] R.P. Feynman, There’s plenty of room at the bottom, *J. Microelectromech. Syst.* (1992).
- [42] T.-C. Lee, et al., Self-Propelling nanomotors in the presence of strong brownian forces, *Nano Lett.* 14 (2014) 2407–2412.
- [43] M. Wan, et al., Systematic research and evaluation models of nanomotors for cancer combined therapy, *Angew. Chem. Int. Ed.* 59 (2020) 14458–14465.
- [44] W. Wang, C. Zhou, A journey of nanomotors for targeted cancer therapy: principles, challenges, and a critical review of the state-of-the-art, *Adv. Healthcare Mater.* 10 (2020).
- [45] T.P. Hoar, J.H. Schulman, Transparent water-in-oil dispersions: the oleopathic hydro-micelle, *Nature* 152 (1943) 102–103.
- [46] C.B. Murray, D.J. Norris, M.G. Bawendi, Synthesis and characterization of nearly monodisperse CdE (E = sulfur, selenium, tellurium) semiconductor nanocrystallites, *J. Am. Chem. Soc.* 115 (1993) 8706–8715.

- [47] M. Bruchez, M. Moronne, P. Gin, S. Weiss, A.P. Alivisatos, Semiconductor nanocrystals as fluorescent biological labels, *Science* 281 (1998) 2013–2016.
- [48] P. Range, et al., Polysorbate-80 coating enhances uptake of polybutylcyanoacrylate (PBCA)-nanoparticles by human and bovine primary brain capillary endothelial cells, *Eur. J. Neurosci.* 12 (2000) 1931–1940.
- [49] Y. Barenholz, Doxil®—the first FDA-approved nano-drug: lessons learned, *J. Contr. Release* 160 (2012) 117–134.
- [50] C.-M.J. Hu, et al., Erythrocyte membrane-camouflaged polymeric nanoparticles as a biomimetic delivery platform, *Proc. Natl. Acad. Sci. U.S.A.* 108 (2011) 10980–10985.
- [51] H. Zhang, Onivyde for the therapy of multiple solid tumors, *Oncotargets Ther.* 9 (2016) 3001–3007.
- [52] K. Bonin, B. Kourmanov, T. Walker, Light torque nanocontrol, nanomotors and nanorockers, *Opt Express* 10 (2002) 984–989.
- [53] W.F. Paxton, et al., Catalytic nanomotors: autonomous movement of striped nanorods, *J. Am. Chem. Soc.* 126 (2004) 13424–13431.
- [54] J. Simmchen, A. Baeza, D. Ruiz, M.J. Esplandiu, M. Vallet-Regí, Asymmetric hybrid silica nanomotors for capture and cargo transport: towards a novel motion-based DNA sensor, *Small* 8 (2012) 2053–2059.
- [55] H.S. Muddana, S. Sengupta, T.E. Mallouk, A. Sen, P.J. Butler, Substrate catalysis enhances single-enzyme diffusion, *J. Am. Chem. Soc.* 132 (2010) 2110–2111.
- [56] M. Wan, et al., Bio-inspired nitric-oxide-driven nanomotor, *Nat. Commun.* 10 (2019) 966.
- [57] S. Ahmed, D.T. Gentekos, C.A. Fink, T.E. Mallouk, Self-assembly of nanorod motors into geometrically regular multimers and their propulsion by ultrasound, *ACS Nano* 8 (2014) 11053–11060.
- [58] M. Liu, et al., Autonomous synergic control of nanomotors, *ACS Nano* 8 (2014) 1792–1803.
- [59] V. Garcia-Gradilla, et al., Ultrasound-propelled nanoporous gold wire for efficient drug loading and release, *Small* 10 (2014) 4154–4159.
- [60] B. Wang, K. Kostarelos, B.J. Nelson, L. Zhang, Trends in micro-/nanorobotics: materials development, actuation, localization, and system integration for biomedical applications, *Adv. Mater.* 33 (2020).
- [61] M. Hu, et al., Micro/nanorobot: a promising targeted drug delivery system, *Pharmaceutics* 12 (2020).
- [62] L. Sonntag, J. Simmchen, V. Magdanz, Nano-and micromotors designed for cancer therapy, *Molecules* 24 (2019).
- [63] J.W. Wang, et al., A self-driven bioreactor based on bacterium-metal-organic framework biohybrids for boosting chemotherapy via cyclic lactate catabolism, *ACS Nano* 15 (2021) 17870–17884.
- [64] L. Yue, et al., Chemotaxis-guided self-propelled macrophage motor for targeted treatment of acute pneumonia, *Adv. Mater.* 35 (2023) e2211626.
- [65] V. Magdanz, et al., IRONSperm: sperm-templated soft magnetic microrobots, *Sci. Adv.* 6 (2020) eaba5855.
- [66] M.B. Akolpoglu, et al., Magnetically steerable bacterial microrobots moving in 3D biological matrices for stimuli-responsive cargo delivery, *Sci. Adv.* 8 (2022).
- [67] S. Erez, E. Karshalev, Y. Wu, J. Wang, G. Yossifon, Electrical propulsion and cargo transport of microbowl shaped Janus particles, *Small* 18 (2022) e2101809.
- [68] M. Lin, et al., A magnetically powered nanomachine with a DNA clutch, *Nat. Nanotechnol.* (2024).
- [69] Y. Wang, et al., NIR-II light powered asymmetric hydrogel nanomotors for enhanced immunochemotherapy, *Angew Chem. Int. Ed. Engl.* 62 (2023) e202212866.
- [70] M. Tang, et al., Polyoxometalate-nanozyme-Integrated nanomotors (POMotors) for self-propulsion-promoted synergistic photothermal-catalytic tumor therapy, *Angew Chem. Int. Ed. Engl.* 63 (2024) e202315031.
- [71] X. Yu, et al., High intensity focused ultrasound-driven nanomotor for effective ferroptosis-immunotherapy of TNBC, *Adv. Sci.* 11 (2024) e2305546.
- [72] G.S. Song, et al., Carbon-coated FeCo nanoparticles as sensitive magnetic-particle-imaging tracers with photothermal and magnetothermal properties, *Nat. Biomed. Eng.* 4 (2020) 325. +.
- [73] M. Zhou, et al., Cancer cell adhesion camouflaged semi-Yolk@Spiky-shell nanomotor for enhanced cell adhesion and synergistic therapy, *Small* 16 (2020).
- [74] M. Tang, et al., Polyoxometalate-nanozyme-Integrated nanomotors (POMotors) for self-propulsion-promoted synergistic photothermal-catalytic tumor therapy, *Angew Chem. Int. Ed. Engl.* (2023) e202315031.
- [75] Z. Zhang, et al., Ultrasound-chargeable persistent luminescence nanoparticles to generate self-propelled motion and photothermal/NO therapy for synergistic tumor treatment, *ACS Nano* 17 (2023) 16089–16106.
- [76] M. Valdez-Garduño, et al., Density asymmetry driven propulsion of ultrasound-powered Janus micromotors, *Adv. Funct. Mater.* 30 (2020).
- [77] Y. Xing, et al., Copper single-atom jellyfish-like nanomotors for enhanced tumor penetration and nanocatalytic therapy, *ACS Nano* 17 (2023) 6789–6799.
- [78] W. Zhang, et al., Micro/nanomotor: a promising drug delivery system for cancer therapy, *ChemPhysMater* 2 (2023) 114–125.
- [79] J.X. Li, et al., Magneto-acoustic hybrid nanomotor, *Nano Lett.* 15 (2015) 4814–4821.
- [80] J.M. McNeill, N. Nama, J.M. Braxton, T.E. Mallouk, Wafer-scale fabrication of micro- to nanoscale bubble swimmers and their fast autonomous propulsion by ultrasound, *ACS Nano* 14 (2020) 7520–7528.
- [81] J. Wang, Z. Xiong, J. Zheng, X. Zhan, J. Tang, Light-driven micro/nanomotor for promising biomedical tools: principle, challenge, and prospect, *Accounts Chem. Res.* 51 (2018) 1957–1965.
- [82] K. Chen, et al., General thermodynamic-controlled coating method to prepare Janus mesoporous nanomotors for improving tumor penetration, *ACS Appl. Mater. Interfaces* 13 (2021) 51297–51311.
- [83] S. Hermanová, M. Pumera, Biocatalytic micro- and nanomotors, *Chem.–Eur. J.* 26 (2020) 11085–11092.
- [84] L.D. Yue, K.K. Yang, J.Y. Li, Q. Cheng, R.B. Wang, Self-propelled asymmetrical nanomotor for self-reported gas therapy, *Small* 17 (2021).
- [85] I.A.B. Pijpers, et al., Hybrid biodegradable nanomotors through compartmentalized synthesis, *Nano Lett.* 20 (2020) 4472–4480.
- [86] S. Gao, et al., Superassembled biocatalytic porous framework micromotors with reversible and sensitive pH-speed regulation at ultralow physiological H<sub>2</sub>O<sub>2</sub> concentration, *Adv. Funct. Mater.* 29 (2019).
- [87] L.L. Wang, et al., Novel catalytic micromotor of porous zeolitic imidazolate framework-67 for precise drug delivery, *Nanoscale* 10 (2018) 11384–11391.
- [88] P. Zhang, et al., Magnetic stomatocyte-like nanomotor as photosensitizer carrier for photodynamic therapy based cancer treatment, *Colloids Surf. B Biointerfaces* 194 (2020).
- [89] D.A. Wilson, R.J.M. Nolte, J.C.M. van Hest, Autonomous movement of platinum-loaded stomatocytes, *Nat. Chem.* 4 (2012) 268–274.
- [90] H. Choi, G.H. Lee, K.S. Kim, S.K. Hahn, Light-guided nanomotor systems for autonomous photothermal cancer therapy, *ACS Appl. Mater. Interfaces* 10 (2018) 2338–2346.
- [91] Y. Tu, et al., Biodegradable hybrid stomatocyte nanomotors for drug delivery, *ACS Nano* 11 (2017) 1957–1963.
- [92] L. Abdelmohsen, et al., Dynamic loading and unloading of proteins in polymeric stomatocytes: formation of an enzyme-loaded supramolecular nanomotor, *ACS Nano* 10 (2016) 2652–2660.
- [93] W. Yu, et al., Self-propelled nanomotor reconstructs tumor microenvironment through synergistic hypoxia alleviation and glycolysis inhibition for promoted anti-metastasis, *Acta Pharm. Sin. B* 11 (2021) 2924–2936.
- [94] M. Zhu, et al., Positive chemotaxis of CREKA-modified Ceria@Polydopamine biomimetic nanoswimmers for enhanced penetration and chemo-photothermal tumor therapy, *ACS Nano* 17 (2023) 17285–17298.
- [95] S. Chen, et al., Dual-source powered nanomotor with integrated functions for cancer photo-theranostics, *Biomaterials* 288 (2022) 121744.
- [96] Q. Li, et al., Nanosized Janus AuNR-Pt motor for enhancing NIR-II photoacoustic imaging of deep tumor and Pt(2+) ion-based chemotherapy, *ACS Nano* 16 (2022) 7947–7960.
- [97] G. Camargo, P.H. Bugatti, P.T.M. Saito, Active semi-supervised learning for biological data classification, *PLoS One* 15 (2020) e0237428.
- [98] Z. Ye, et al., Supramolecular modular assembly of imaging-trackable enzymatic nanomotors, *Angew Chem. Int. Ed. Engl.* 63 (2024) e202401209.
- [99] A.C. Hortelão, R. Carrasqueira, N. Murillo-Cremaes, T. Patiño, S. Sánchez, Targeting 3D bladder cancer spheroids with urease-powered nanomotors, *ACS Nano* 13 (2019) 429–439.
- [100] H. Choi, S.H. Cho, S.K. Hahn, Urease-powered polydopamine nanomotors for intravesical therapy of bladder diseases, *ACS Nano* 14 (2020) 6683–6692.
- [101] Z. Yang, et al., Ultrasmall enzyme-powered Janus nanomotor working in blood circulation system, *ACS Nano* 17 (2023) 6023–6035.
- [102] D. Xu, et al., Enzyme-powered liquid metal nanobots endowed with multiple biomedical functions, *ACS Nano* 15 (2021) 11543–11554.
- [103] X. Arqué, et al., Autonomous treatment of bacterial infections in vivo using antimicrobial micro- and nanomotors, *ACS Nano* 16 (2022) 7547–7558.
- [104] X. Liu, et al., Urease-powered micromotors with spatially selective distribution of enzymes for capturing and sensing exosomes, *ACS Nano* 17 (2023) 24343–24354.
- [105] Z. Zhang, et al., Icebreaker-inspired Janus nanomotors to combat barriers in the delivery of chemotherapeutic agents, *Nanoscale* 13 (2021) 6545–6557.
- [106] J. Zheng, R. Qi, C. Dai, G. Li, M. Sang, Enzyme catalysis biomotor engineering of neutrophils for nanodrug delivery and cell-based thrombolytic therapy, *ACS Nano* 16 (2022) 2330–2344.
- [107] M.M. Wan, et al., Nitric oxide-driven nanomotor for deep tissue penetration and multidrug resistance reversal in cancer therapy, *Adv. Sci.* 8 (2021) 2002525.
- [108] H. Chen, et al., Deep penetration of nanolevel drugs and micrometer-level T cells promoted by nanomotors for cancer immunochemotherapy, *J. Am. Chem. Soc.* 143 (2021) 12025–12037.
- [109] T. Li, et al., A universal chemotactic targeted delivery strategy for inflammatory diseases, *Adv. Mater.* 34 (2022) e2206654.
- [110] X. Tang, et al., Lipophilic NO-driven nanomotors as drug balloon coating for the treatment of atherosclerosis, *Small* 19 (2023) e2203238.
- [111] H. Wang, et al., Dual-fuel propelled nanomotors with two-stage permeation for deep bacterial infection in the treatment of pulpitis, *Adv. Sci.* (2023) e2305063.
- [112] Z. Wu, et al., Carrier-free trehalose-based nanomotors targeting macrophages in inflammatory plaque for treatment of atherosclerosis, *ACS Nano* 16 (2022) 3808–3820.
- [113] J. Zheng, et al., Cascade catalytically released nitric oxide-driven nanomotor with enhanced penetration for antibiofilm, *Small* 18 (2022) e2205252.
- [114] M. Liu, et al., Enzyme-based mesoporous nanomotors with near-infrared optical brakes, *J. Am. Chem. Soc.* 144 (2022) 3892–3901.
- [115] J. Yu, et al., Self-propelled enzymatic nanomotors from prodrug-skeletal zeolitic imidazolate frameworks for boosting multimodal cancer therapy efficiency, *Adv. Sci.* 10 (2023) e2301919.
- [116] T. Zhang, et al., Photothermal-triggered sulfur oxide gas therapy augments type I photodynamic therapy for potentiating cancer stem cell ablation and inhibiting radioresistant tumor recurrence, *Adv. Sci.* 10 (2023) e2304042.
- [117] F. Moradi Kashkooli, M. Soltani, M. Souri, Controlled anti-cancer drug release through advanced nano-drug delivery systems: static and dynamic targeting strategies, *J. Contr. Release* 327 (2020) 316–349.
- [118] M. Damaghi, et al., The harsh microenvironment in early breast cancer selects for a Warburg phenotype, *Proc. Natl. Acad. Sci. U. S. A.* 118 (2021).

- [119] M. Luo, Y. Feng, T. Wang, J. Guan, Micro-/Nanorobots at work in active drug delivery, *Adv. Funct. Mater.* 28 (2018).
- [120] X. Zhan, et al., Enhanced ion tolerance of electrokinetic locomotion in polyelectrolyte-coated microswimmer, *Nat. Commun.* 10 (2019) 3921.
- [121] C. Simó, et al., Urease-powered nanobots for radionuclide bladder cancer therapy, *Nat. Nanotechnol.* (2024).
- [122] A.C. Hortelao, et al., Swarming behavior and in vivo monitoring of enzymatic nanomotors within the bladder, *Sci. Robot.* 6 (2021).
- [123] M. Yang, et al., Swarming magnetic nanorobots bio-interfaced by heparinoid-polymer brushes for in vivo safe synergistic thrombolysis, *Sci. Adv.* 9 (2023) eadk7251.
- [124] J. Hu, et al., Engineering macromolecular nanocarriers for local delivery of gaseous signaling molecules, *Adv. Drug Deliv. Rev.* 179 (2021) 114005.
- [125] W. Fan, B.C. Yung, X. Chen, Stimuli-responsive NO release for on-demand gas-sensitized synergistic cancer therapy, *Angew. Chem. Int. Ed. Engl.* 57 (2018) 8383–8394.
- [126] Y. Liu, et al., Sphingosine 1-phosphate liposomes for targeted nitric oxide delivery to mediate anticancer effects against brain glioma tumors, *Adv. Mater.* 33 (2021) e2101701.
- [127] Z. Zhao, et al., Nitric oxide-driven nanotherapeutics for cancer treatment, *J. Contr. Release* 362 (2023) 151–169.
- [128] J. Hou, et al., Targeted delivery of nitric oxide via a 'bump-and-hole'-based enzyme-prodrug pair, *Nat. Chem. Biol.* 15 (2019) 151–160.
- [129] L.B. Vong, Y. Nagasaki, Nitric oxide nano-delivery systems for cancer therapeutics: advances and challenges, *Antioxidants* 9 (2020).
- [130] X. Dong, et al., Enhanced drug delivery by nanoscale integration of a nitric oxide donor to induce tumor collagen depletion, *Nano Lett.* 19 (2019) 997–1008.
- [131] T.C. Lee, et al., Self-propelling nanomotors in the presence of strong Brownian forces, *Nano Lett.* 14 (2014) 2407–2412.
- [132] W. Kim, et al., Protein corona: friend or foe? Co-opting serum proteins for nanoparticle delivery, *Adv. Drug Deliv. Rev.* 192 (2023) 114635.
- [133] A. Salvati, et al., Transferrin-functionalized nanoparticles lose their targeting capabilities when a biomolecule corona adsorbs on the surface, *Nat. Nanotechnol.* 8 (2013) 137–143.
- [134] E. Casals, T. Pfaller, A. Duschl, G.J. Oostingh, V. Puentes, Time evolution of the nanoparticle protein corona, *ACS Nano* 4 (2010) 3623–3632.
- [135] M. Hadjide metriou, et al., The human in vivo biomolecule corona onto PEGylated liposomes: a proof-of-concept clinical study, *Adv. Mater.* 31 (2019) e1803335.
- [136] J.L. Perry, et al., PEGylated PRINT nanoparticles: the impact of PEG density on protein binding, macrophage association, biodistribution, and pharmacokinetics, *Nano Lett.* 12 (2012) 5304–5310.
- [137] R. Yang, et al., Cancer cell membrane-coated adjuvant nanoparticles with mannose modification for effective anticancer vaccination, *ACS Nano* 12 (2018) 5121–5129.
- [138] Z. Cao, et al., Biomimetic macrophage membrane-camouflaged nanoparticles induce ferroptosis by promoting mitochondrial damage in glioblastoma, *ACS Nano* 17 (2023) 23746–23760.
- [139] W. Wang, Open questions of chemically powered nano- and micromotors, *J. Am. Chem. Soc.* 145 (2023) 27185–27197.
- [140] W. Wang, W. Duan, S. Ahmed, T.E. Mallouk, A. Sen, Small power: autonomous nano- and micromotors propelled by self-generated gradients, *Nano Today* 8 (2013) 531–554.
- [141] G. Yuan, et al., Modulating intracellular dynamics for optimized intracellular release and transcytosis equilibrium, *Adv. Mater.* (2024) e2400425.
- [142] C. Lin, et al., Biodegradable calcium sulfide-based nanomodulators for H(2)S-boosted Ca(2+)-involved synergistic cascade cancer therapy, *Acta Pharm. Sin.* 12 (2022) 4472–4485.
- [143] B. Li, et al., Photothermal therapy of tuberculosis using targeting pre-activated macrophage membrane-coated nanoparticles, *Nat. Nanotechnol.* (2024).
- [144] S. Feng, et al., Synergistic anti-tumor therapy by a homotypic cell membrane-coated biomimetic nanocarrier with exceptionally potent activity against hepatic carcinoma, *Nano Res.* 15 (2022) 8255–8269.